

Origin and Characterization of Eagle Ford Pore Networks in the South Texas Upper Cretaceous Shelf*

Lucy Tingwei Ko^{1,2}, Robert G. Loucks², Stephen C. Ruppel², Tongwei Zhang², and Sheng Peng²

Search and Discovery Article #51281 (2016)**

Posted August 8, 2016

*Adapted from oral presentation given at AAPG 2016 Annual Convention and Exhibition, Calgary, Alberta, Canada, June 19-22, 2016

**Datapages © 2016 Serial rights given by author. For all other rights contact author directly.

¹Department of Geological Sciences, The University of Texas at Austin, Austin, Texas, United States (tingwei.ko@utexas.edu)

²Bureau of Economic Geology, The University of Texas at Austin, Austin, Texas, United States

Abstract

Recent studies have demonstrated that loss of primary pores and development of secondary pores in mudrocks are primarily controlled by burial diagenesis of the sediments and thermal maturation of organic matter. Lack of quantitative data on micro- to nanometer rock properties, however, limits the ability to understand and predict petrophysical properties and fluid flow in these fine-grained rocks. To upscale these rock properties requires detailed quantification of the pore types and distribution at multiple scales. Upper Cretaceous Eagle Ford mudstone samples were collected from continuous cores taken from two adjacent (~6 km) oil-producing wells in Karnes County, Texas to investigate small-scale variations in mineralogy, diagenesis, and pore types. Backscattered and secondary electron images were collected at 5,000X, 15,000X, and 120,000X (instrument magnification) using a field-emission scanning electron microscope (FE-SEM) to capture a broad range of visible pore sizes and pore distribution. Consistent point-count methods were used to systematically quantify pore types. Pore-tracing methods were used to validate point-count methods as well as to provide size and shape information of the organic-matter (OM) pores and mineral pores. Eagle Ford facies in the studied include: (1) thin ash beds, (2) globigerinid-bearing, laminated, argillaceous wackestone-packstone (marl) with varying organic matter content, and (3) lime packstone with varying calcite, quartz, and clay mineral content. Samples from the two cores show similar thermal maturity histories. Pores include both secondary OM pores in migrated solid bitumen and primary interparticle pores between coccolith elements (with residual OM). The Eagle Ford mineral pore network consists of mineral pores originally saturated with formation water and partly cemented mineral pores containing migrated bitumen with OM pores. SEM-image-based point-count porosity data show that Eagle Ford pore network in both wells is dominated by primary mineral pores, but that secondary OM pores in migrated bitumen are also important. This study

concludes that the reservoir quality of Eagle Ford mudstones varies significantly at similar levels of thermal maturation. Pore morphology, TOC, and mineralogy all impact total porosity. A positive correlation was found between the amount of OM porosity and TOC, and between mineral porosity and volume percentage of quartz and feldspar.

References Cited

Afsharpoor, A., and F. Javadpour, 2016, Liquid Slip Flow in a Network of Shale Noncircular Nanopores: *Fuel*, v. 180, p. 580-590. doi:10.1016/j.fuel.2016.04.078

Ko, L.T., T. Zhang, R.G. Loucks, S.C. Ruppel, and Deyong Shao, 2016, Pore Evolution in the Barnett, Eagle Ford (Boquillas), and Woodford Mudrocks Based on Gold-Tube Pyrolysis Thermal Maturation: AAPG 2015 Annual Convention and Exhibition, Denver, Colorado, May 31 – June 3, 2015, Search and Discovery Article #51228 (2016), http://www.searchanddiscovery.com/documents/2016/51228ko/ndx_ko.pdf, Web accessed August 2016.

Loucks, R.G., R.M. Reed, S.C. Ruppel, and U. Hammes, 2012, Spectrum of Pore Types and Networks in Mudrocks and a Descriptive Classification for Matrix-Related Mudrock Pores: *AAPG Bulletin*, v. 96, p. 1071-1098.

Roduit, N., 2008, JMicroVision: Image Analysis Toolbox for Measuring and Quantifying Components of High-Definition Images, Version 1.2.7. Software available for free download at <http://www.jmicrovision.com/> Web accessed August 2016.

Ruppel, S.C., R.G. Loucks, and G. Frébourg, 2012, Guide to Field Exposures of the Eagle Ford-Equivalent Boquillas Formation and Related Upper Cretaceous Units in Southwest Texas: The University of Texas at Austin, Bureau of Economic Geology, Mudrock Systems Research Laboratory Field-Trip Guidebook, 151 p.

Origin and Characterization of Eagle Ford Pore Networks in the South Texas Upper Cretaceous Shelf

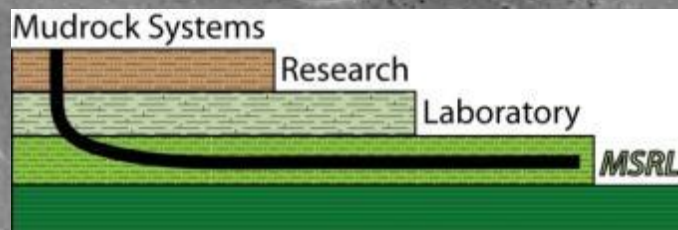
**Lucy T. Ko, Bob Loucks, Steve Ruppel,
Tongwei Zhang, and Sheng Peng**

Presentation date: June 20th, 2016

AAPG Annual Convention & Exhibition, Calgary, Canada



**BUREAU OF
ECONOMIC
GEOLOGY**

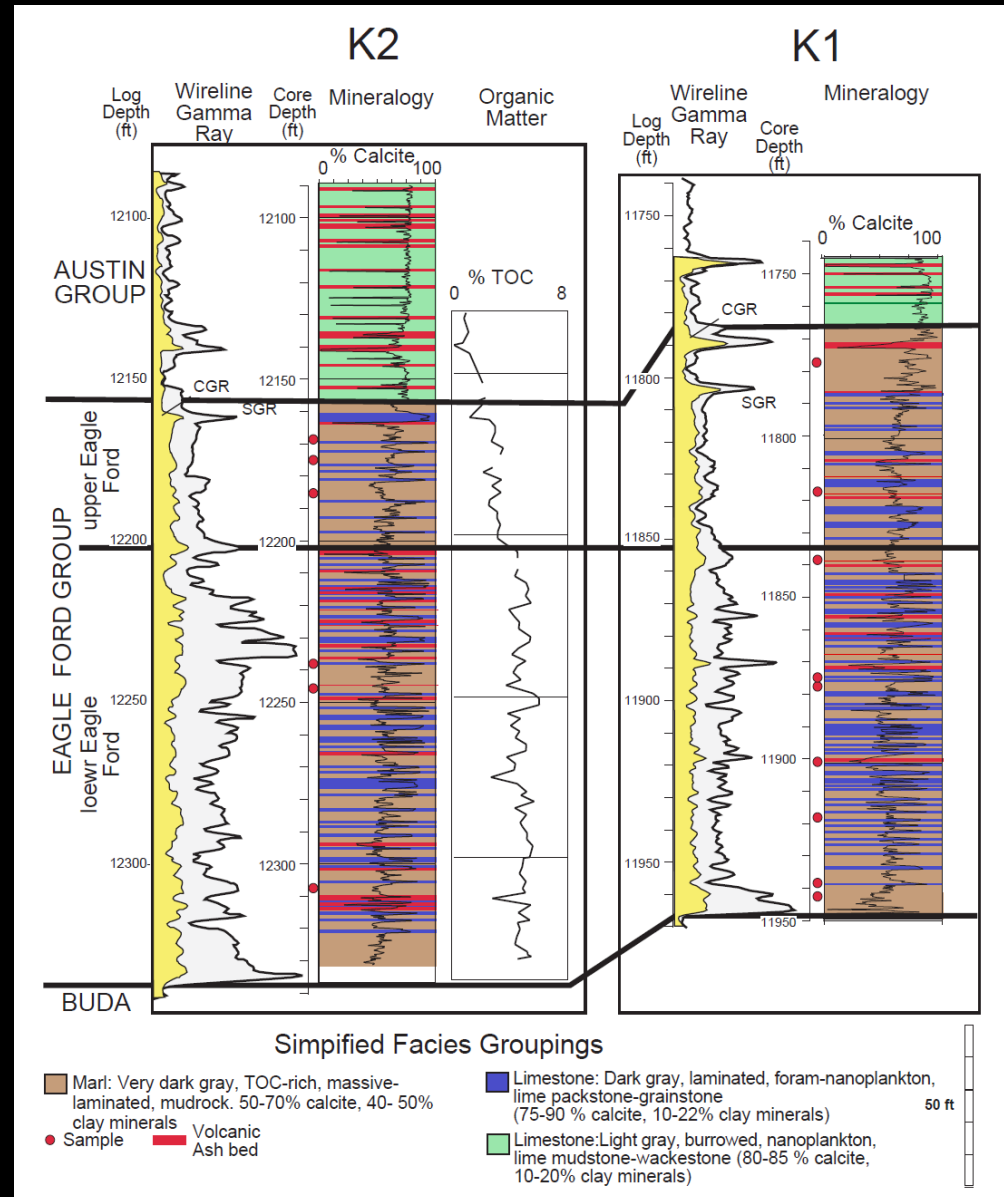


TEXAS Geosciences

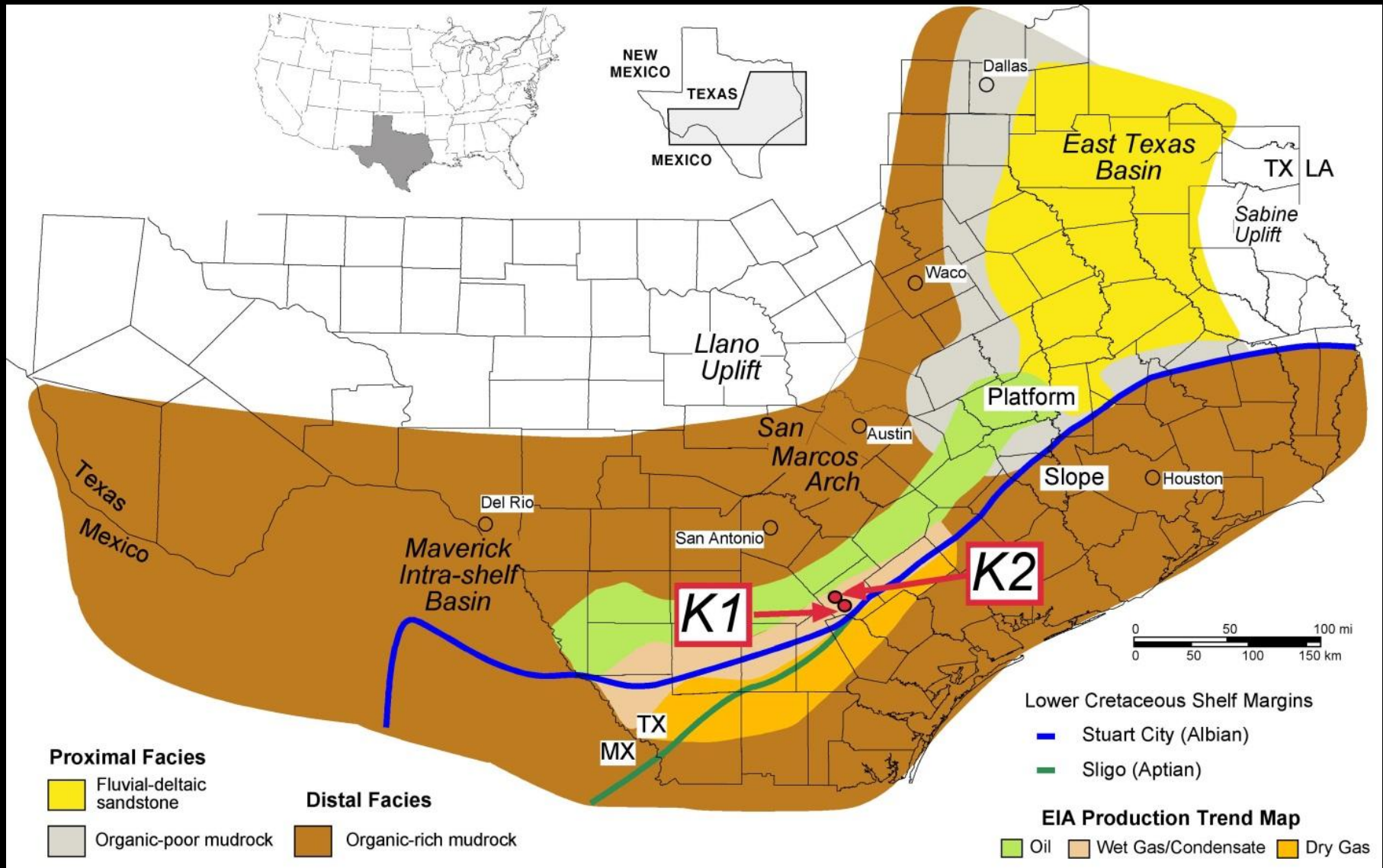
The University of Texas at Austin
Jackson School of Geosciences

Sample Location and Depth

- K1 and K2 wells are about 4 miles apart
- K2 well is slightly deeper than K1 well
- Samples were selected based on lithofacies defined by core description and XRF
- 9 samples from K1; 7 samples from K2
- 13 marl samples; 3 limestone samples
- Division of UEF and LEF is based on U abundance from spectral GR, corresponding to changes in TOC and [Mo]
- UEF: marls with less TOC, ash beds uncommon
- LEF: marls with high TOC, ash beds common



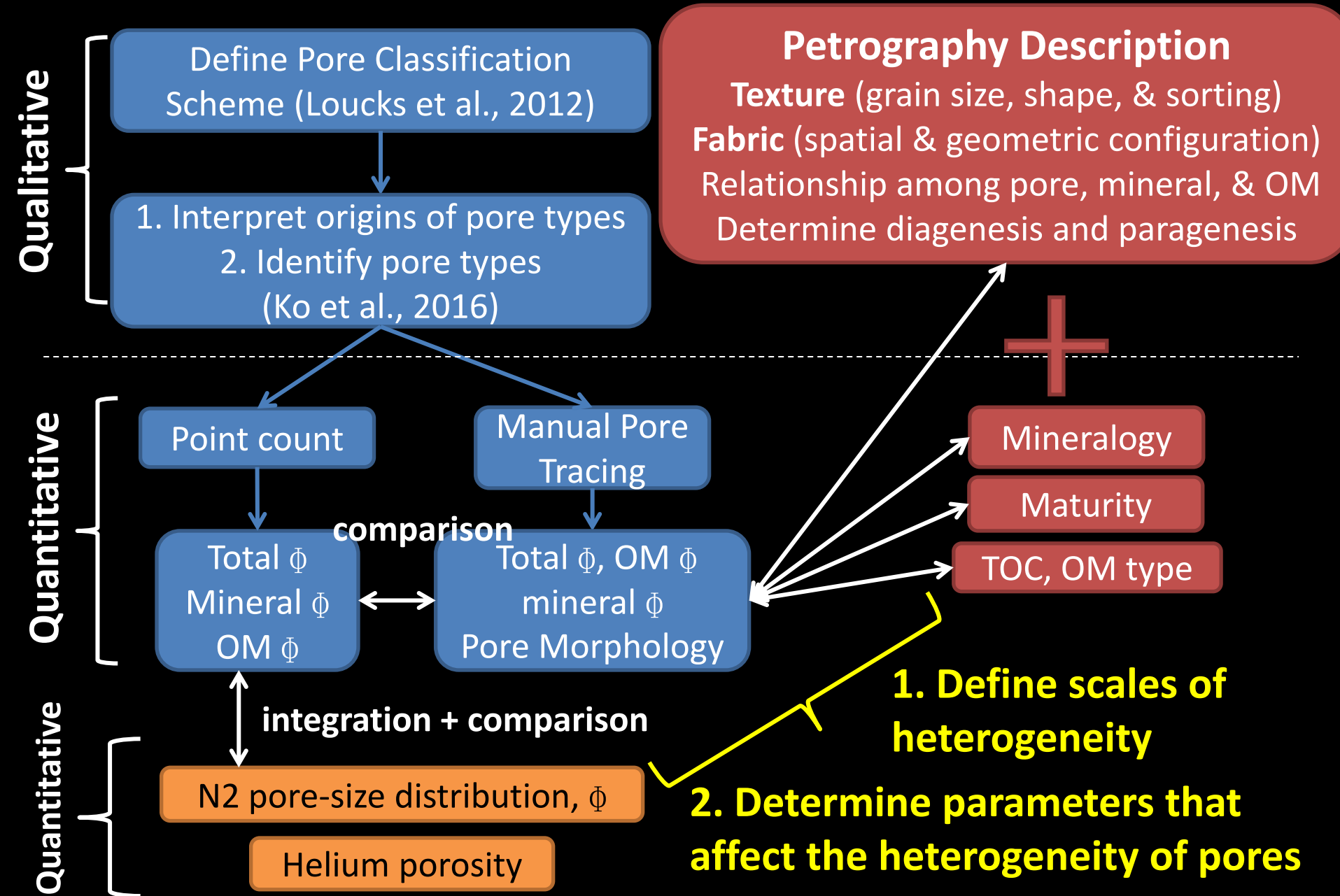
Sample Location and Depth



Motivation and Research Question

- Lack of quantitative data on micron- to nanometer-scale rock properties has limited the ability to define and predict petrophysical properties and fluid transport mechanism.
- SEM image-based porosity and pore-size distribution vs. nitrogen adsorption vs. helium pycnometry
- Dominant pore type and pore network in the Eagle Ford?
- What controls pore types and their size distribution?
- In addition to thermal maturity, what else can impact pore type, abundance, and distribution?

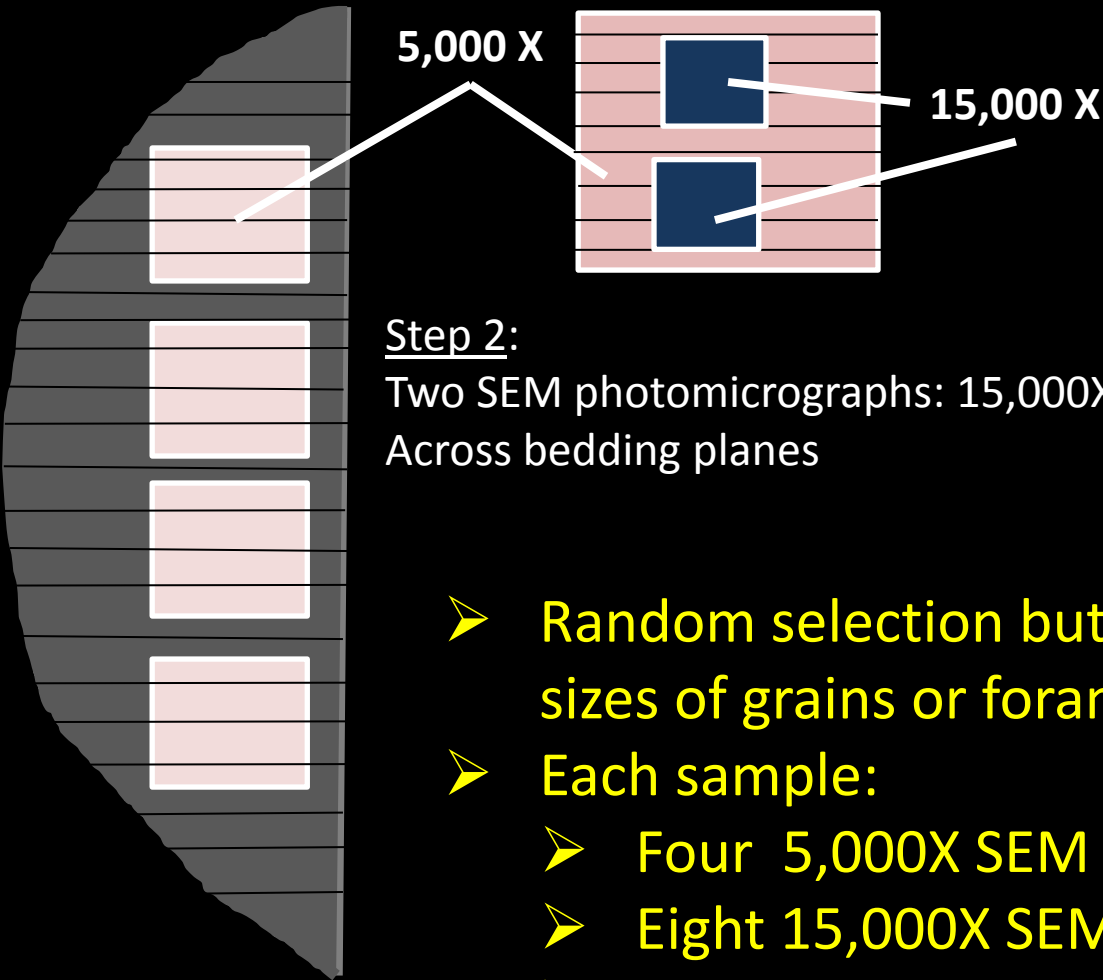
Research Objectives and Workflow



Methods: Three Scales of Investigation

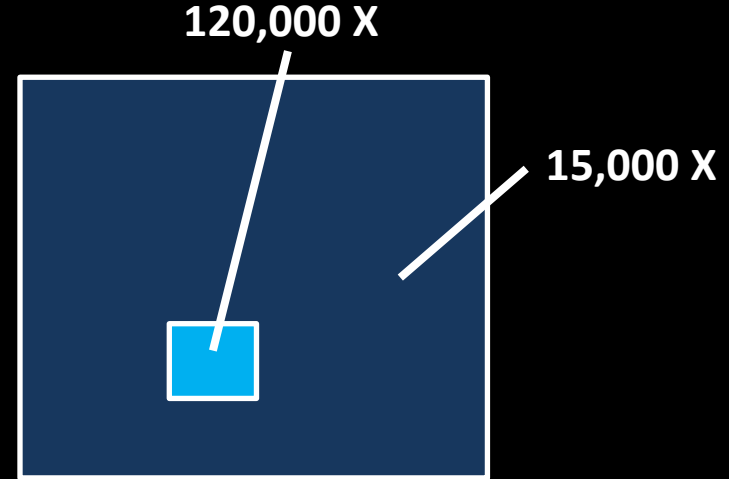
Step 1:

Four SEM photomicrographs: 5,000X
randomly selected, across bedding



Step 2:

Two SEM photomicrographs: 15,000X
Across bedding planes



Step 3:

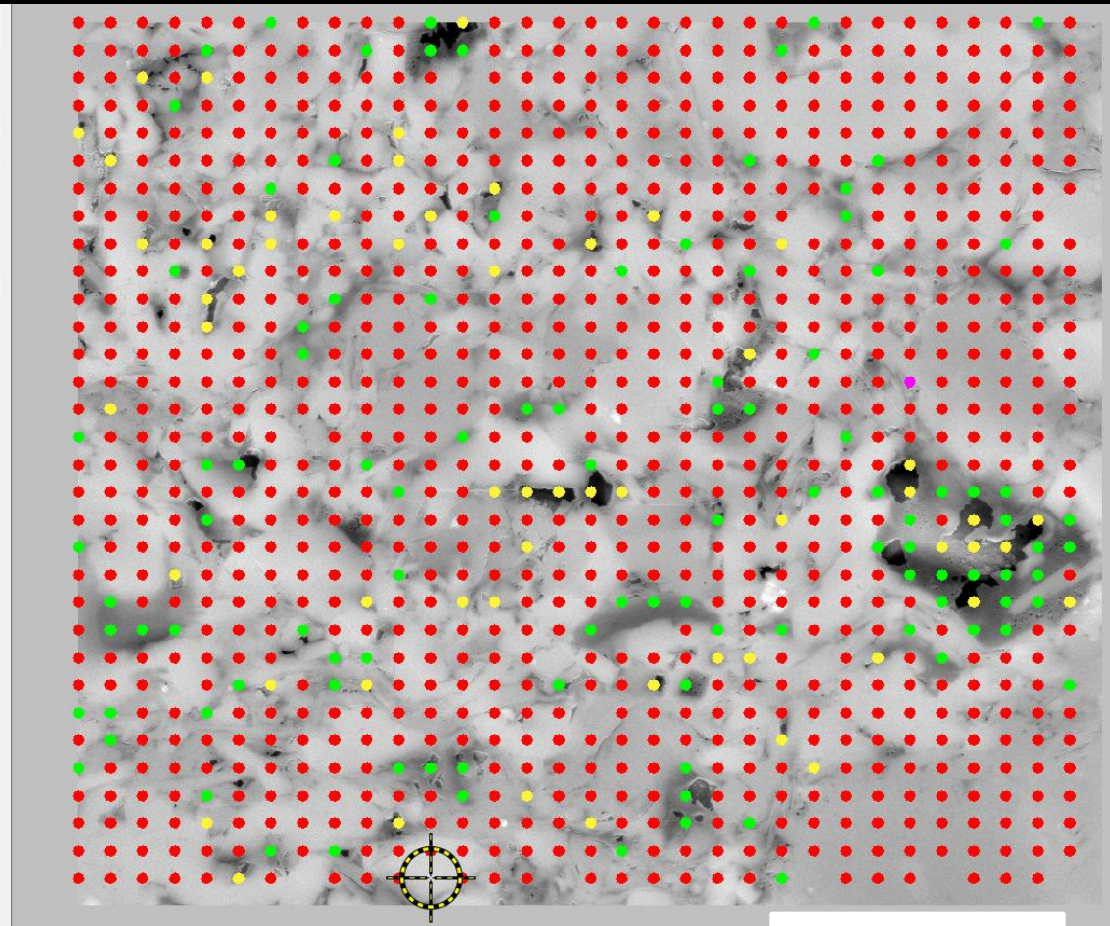
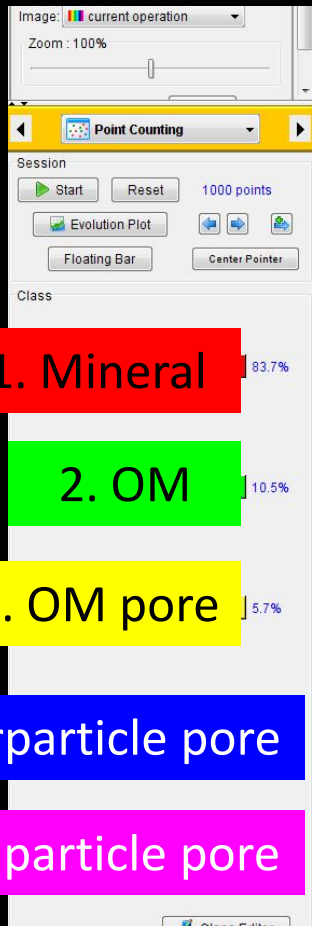
1 SEM photomicrographs: 120,000X
Focus on OM pores
One inside foram
Another one in the matrix

- Random selection but avoid anomalously large sizes of grains or forams
- Each sample:
 - Four 5,000X SEM photos
 - Eight 15,000X SEM photos
 - Eight 120,000X SEM photos

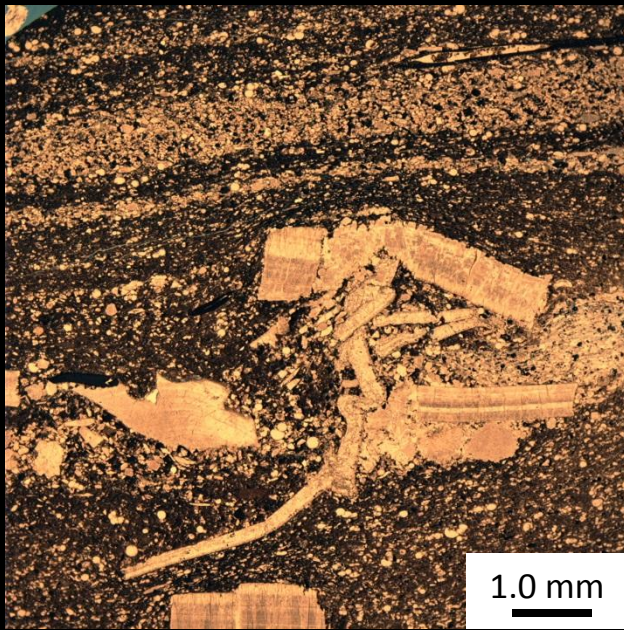
Methods – Point Count vs. Pore Tracing

Five categories : Mineral, OM, OM pore, interP pore, intraP pore

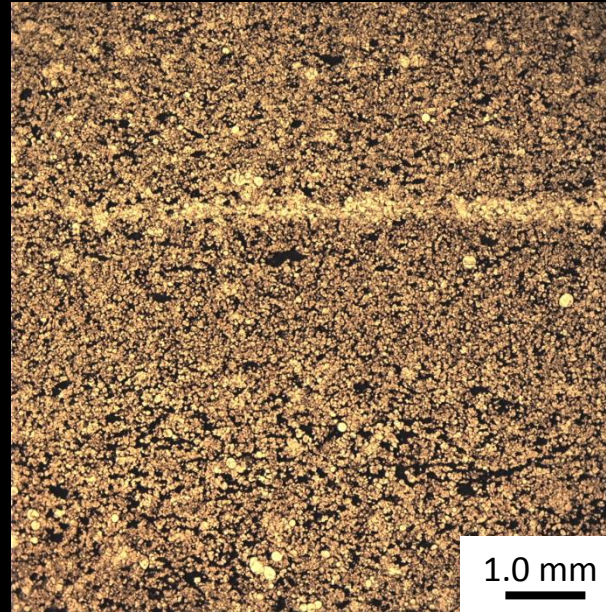
Total counted points: 1,000 points; *JMicrovision* (Roduit, 2008)



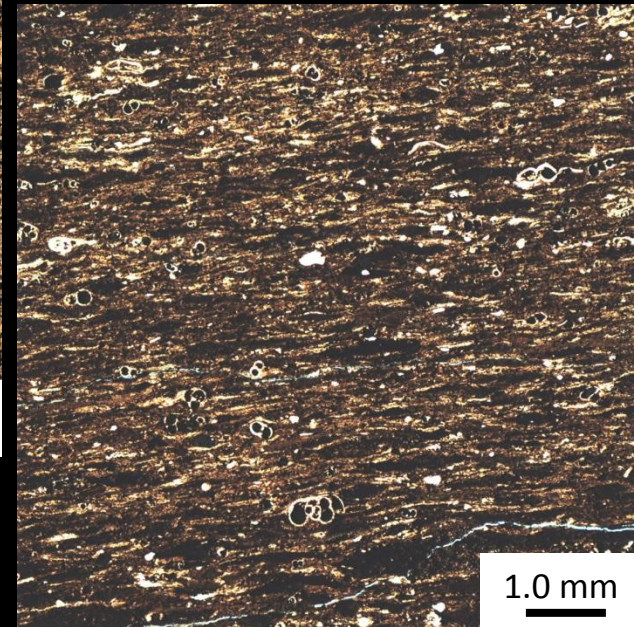
Lithofacies



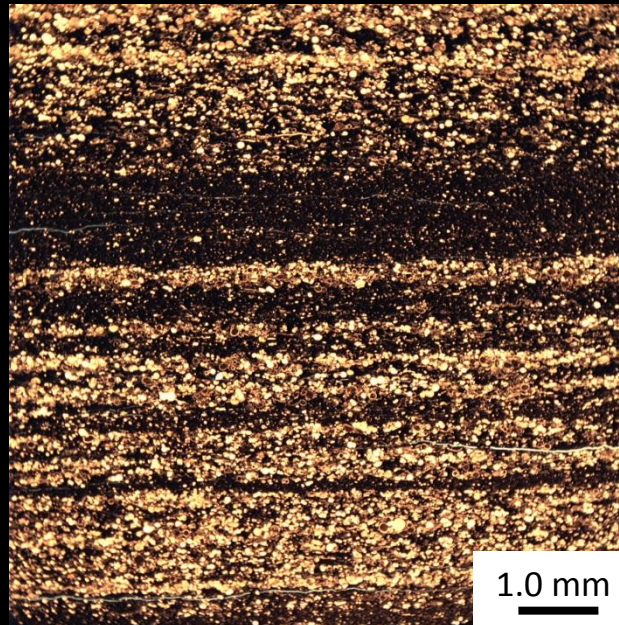
1. Skeletal-debris,
globigerinid-bearing,
laminated
wackestone-packstone



2. Globigerinid-bearing,
laminated packstone

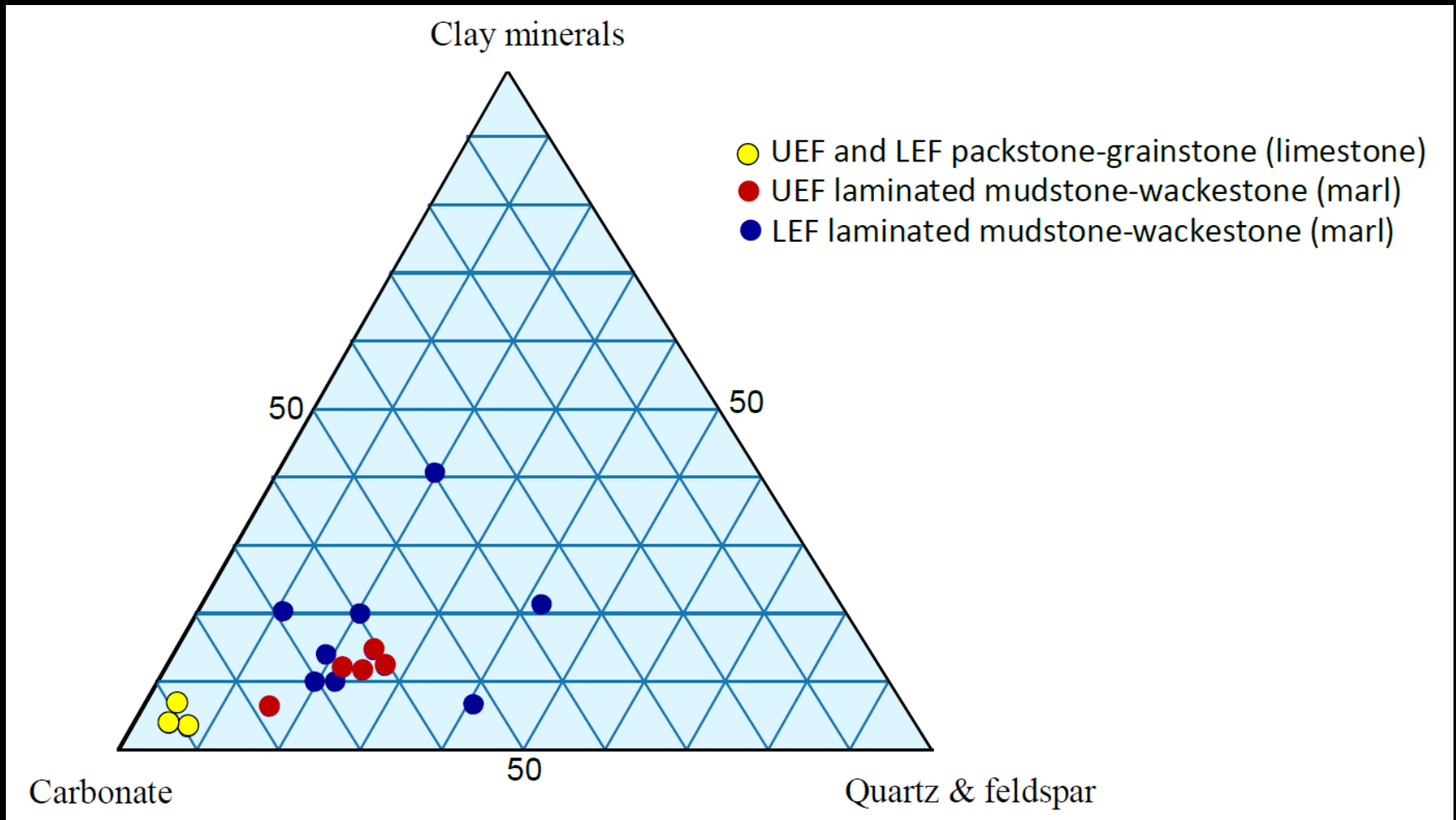


4. Globigerinid-bearing,
laminated
mudstone-wackestone



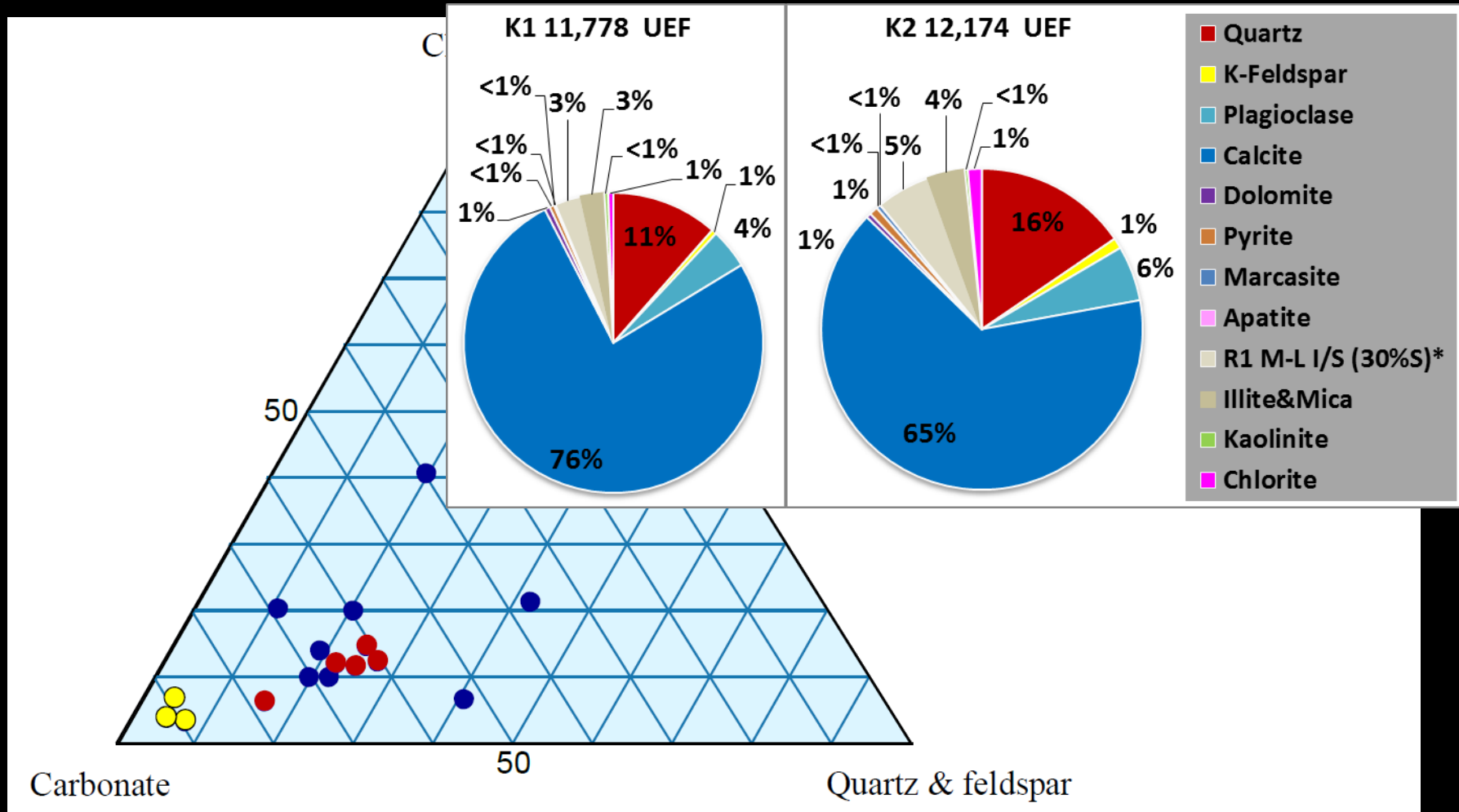
3. Globigerinid-bearing,
laminated
wackestone-packstone

Bulk Mineralogy – UEF & LEF Marl, Limestone

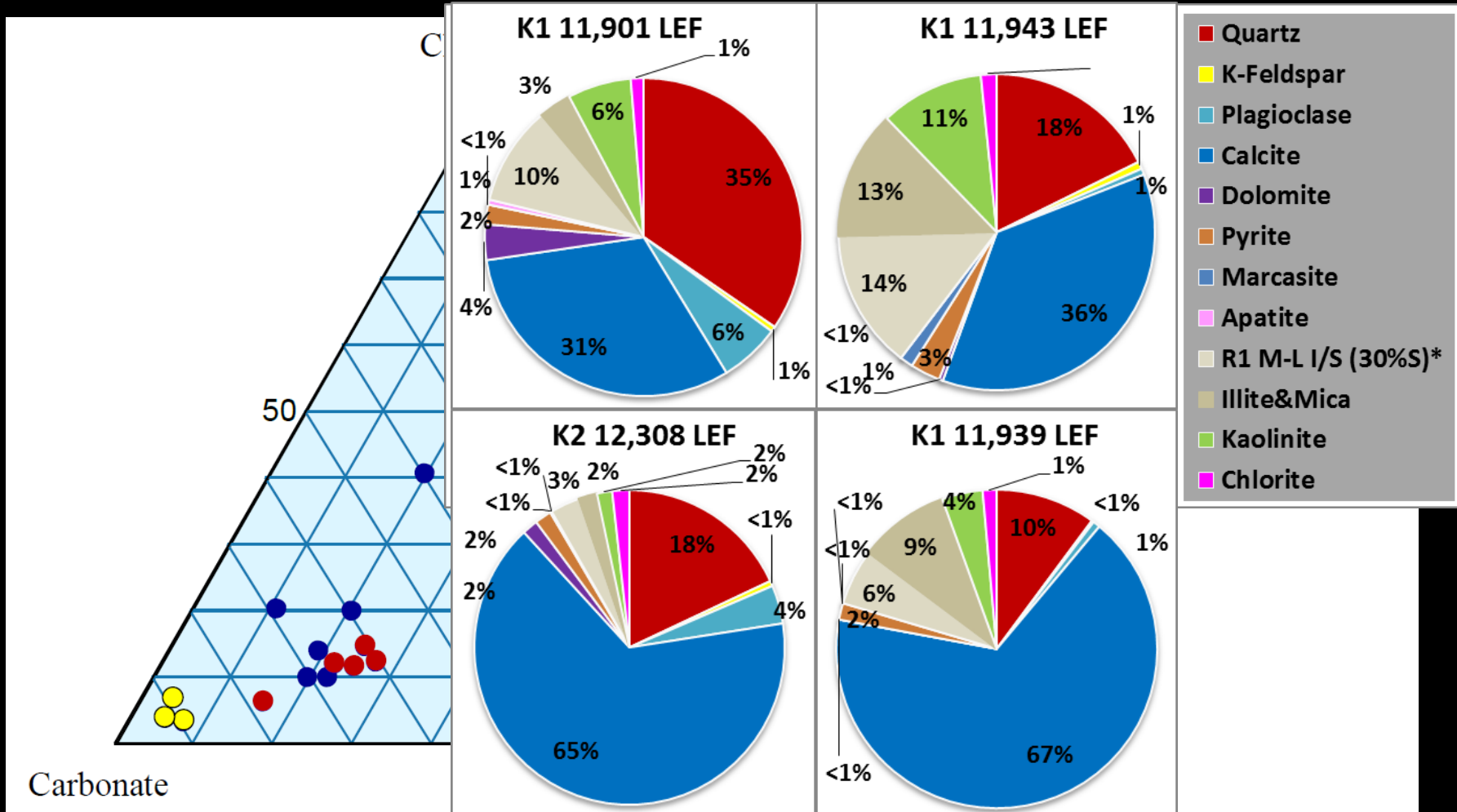


- Increasing amount of kaolinite and chlorite from upper to lower EF.

Bulk Mineralogy – UEF & LEF Marl, Limestone

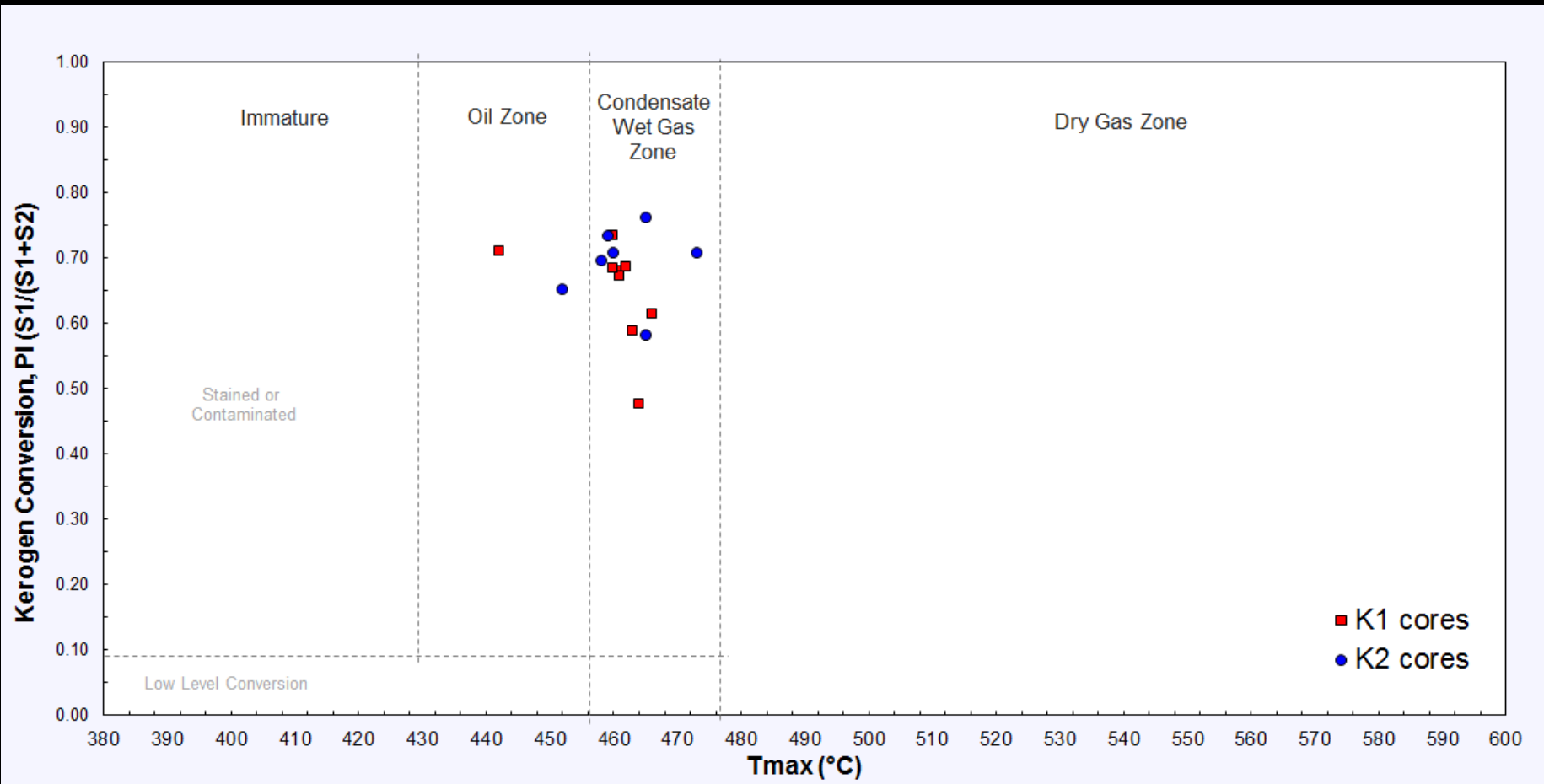


Bulk Mineralogy – UEF & LEF Marl, Limestone



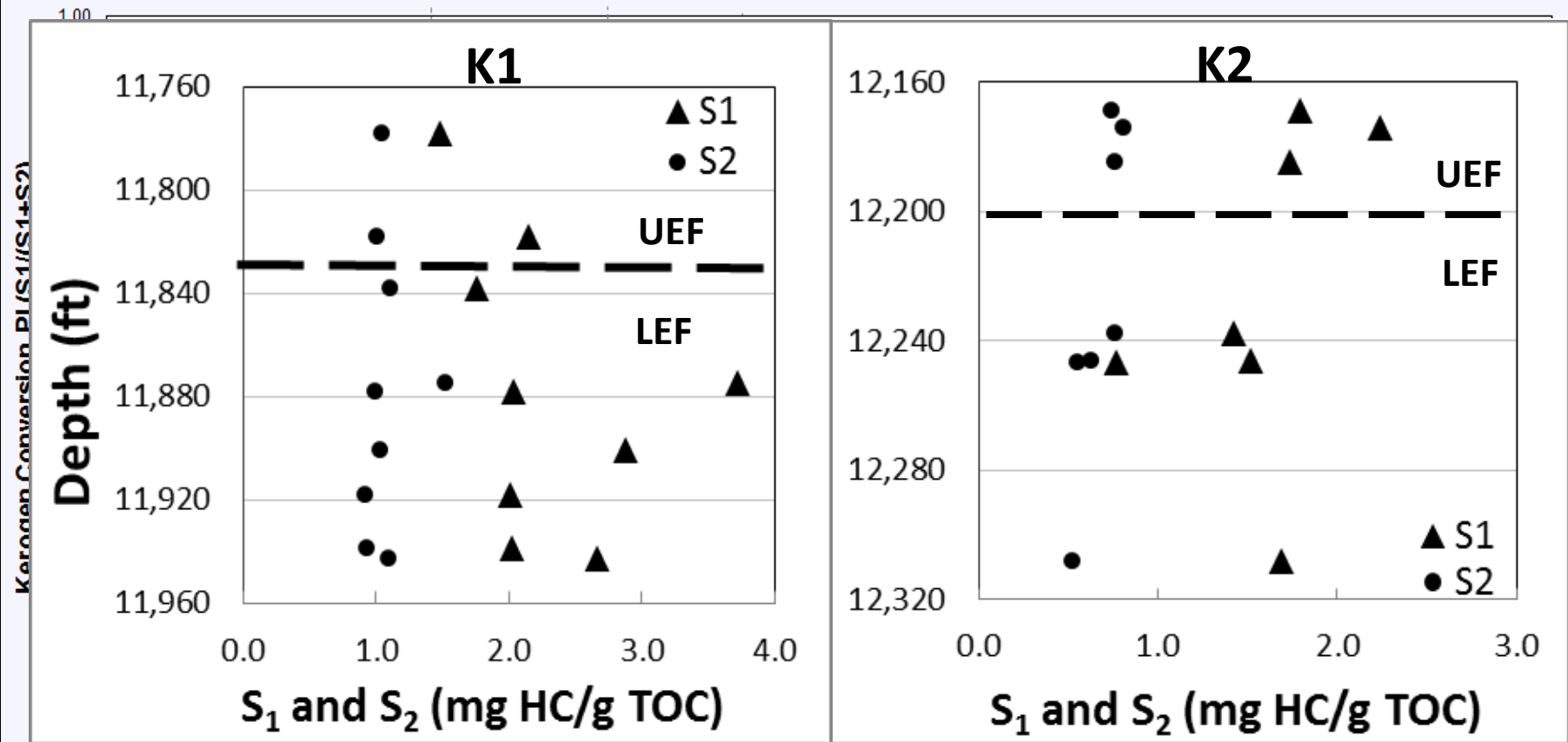
- Increasing amount of kaolinite and chlorite from upper to lower EF.

Geochemical Properties: TOC, Maturity



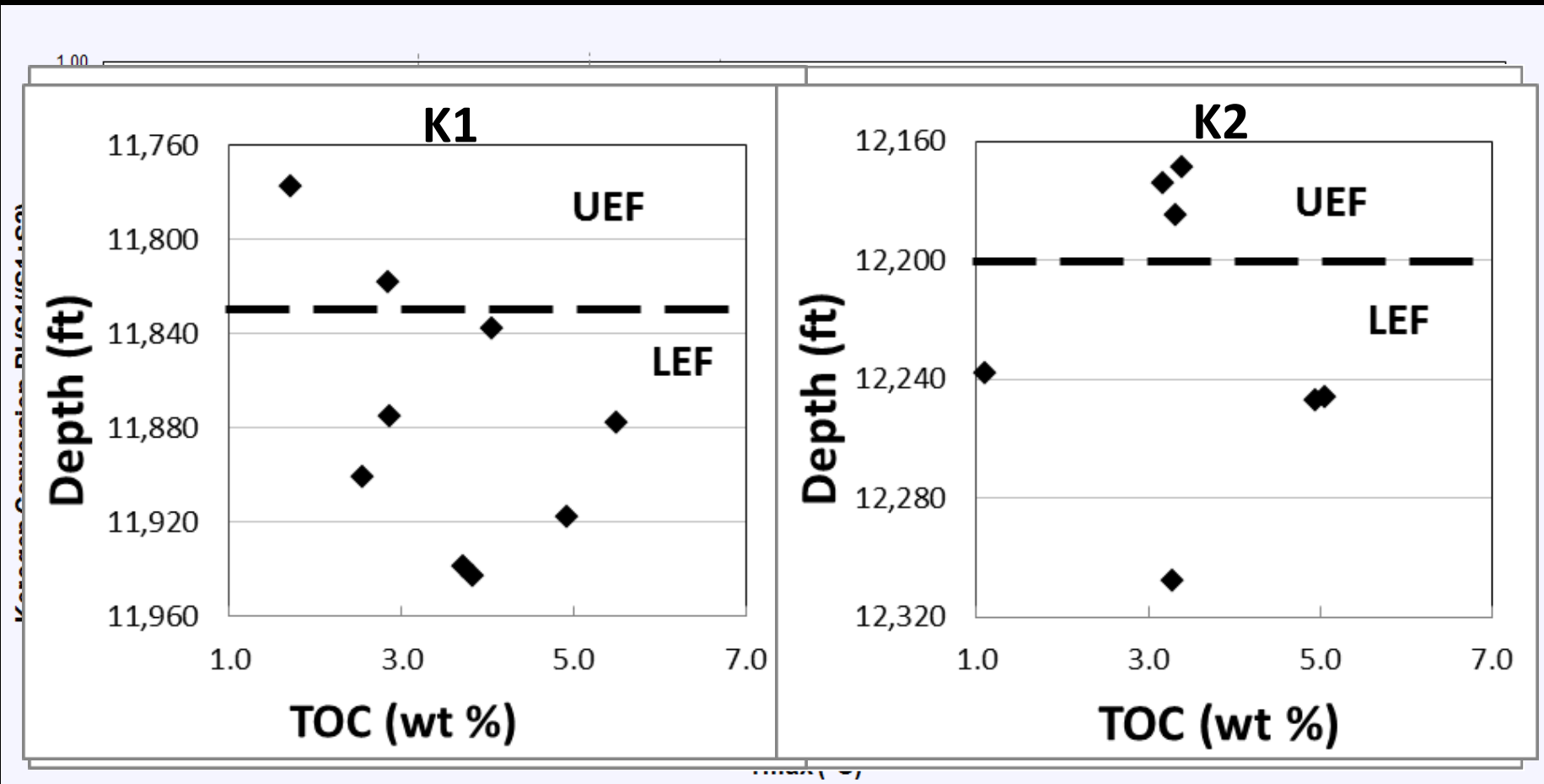
- EF samples have reached late oil to condensate and gas window

Geochemical Properties: TOC, Maturity



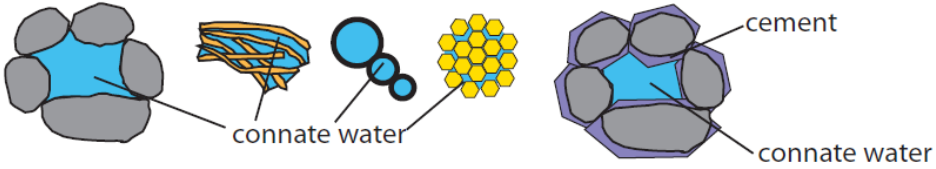
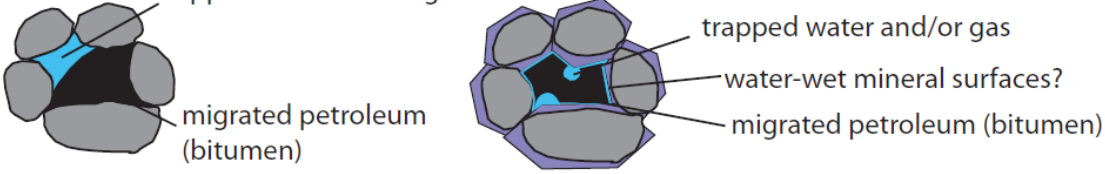
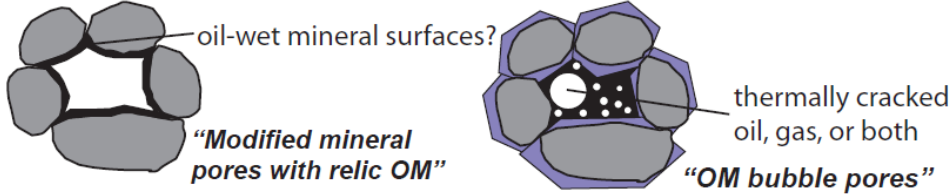
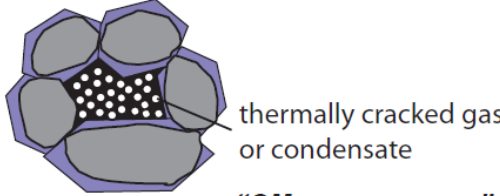
- EF samples have reached late oil to condensate and gas window
- K2 cores slightly more mature than K1 cores

Geochemical Properties: TOC, Maturity



- EF samples have reached late oil to condensate and gas window
- K2 cores slightly more mature than K1 cores

Eagle Ford Pore Evolution Model

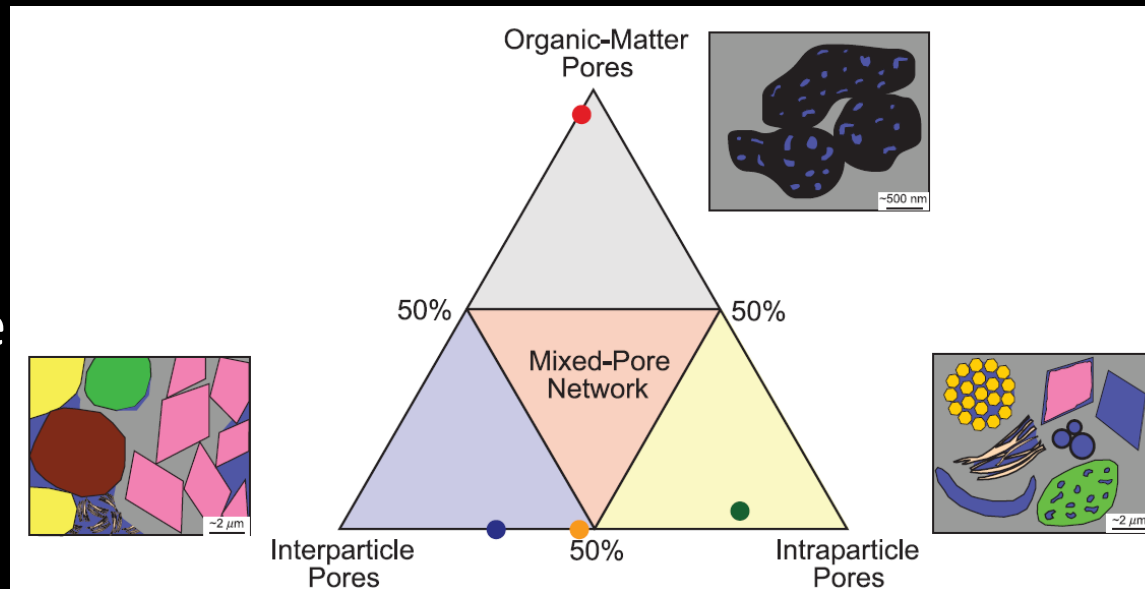
Petroleum generation stage	Organic matter	Minerals and pore types of Eagle Ford marine mudrocks
Kerogen ↓		 <p><i>"Primary mineral pores"</i></p>
↓ Bitumen + gas ↓		 <p><i>"Modified mineral pores with relic OM"</i></p>
↓ Oil + gas ↓		 <p><i>"Modified mineral pores with relic OM"</i> <i>"OM bubble pores"</i></p>
↓ Gas	↓ decrease in volume of kerogen	 <p><i>"OM spongy pores"</i></p>

(Ko et al., 2016, in press)

Define and Categorize EF Pore Types

- **Mineral pores**
 - Primary mineral pore
 - Interparticle pore
 - Intraparticle pore
 - Modified mineral pore

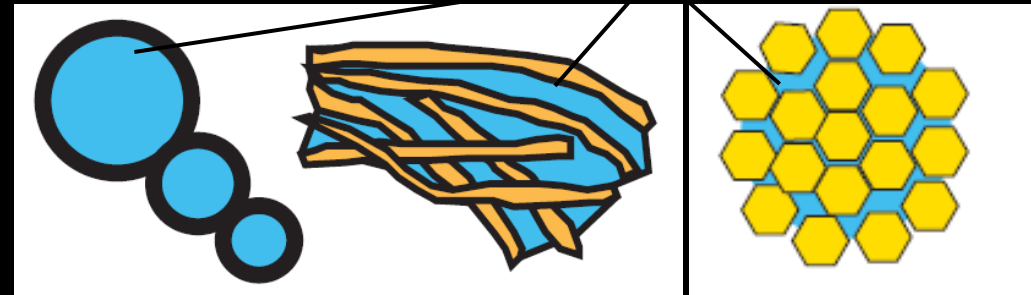
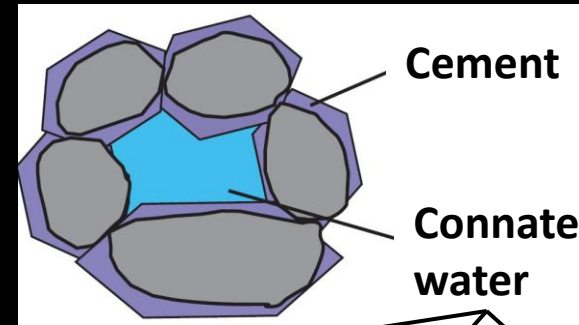
- **OM pores**
 - Primary OM pore
 - Secondary OM pore
 - OM bubble pore
 - OM spongy pore



Define and Categorize EF Pore Types

- **Mineral pores**

- Primary mineral pore
 - Interparticle pore
 - Intraparticle pore
- Modified mineral pore



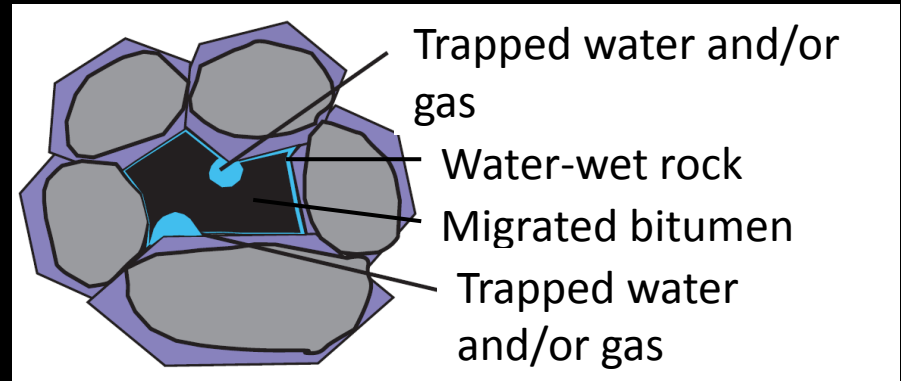
- **OM pores**

- Primary OM pore
- Secondary OM pore
 - OM bubble pore
 - OM spongy pore

Define and Categorize EF Pore Types

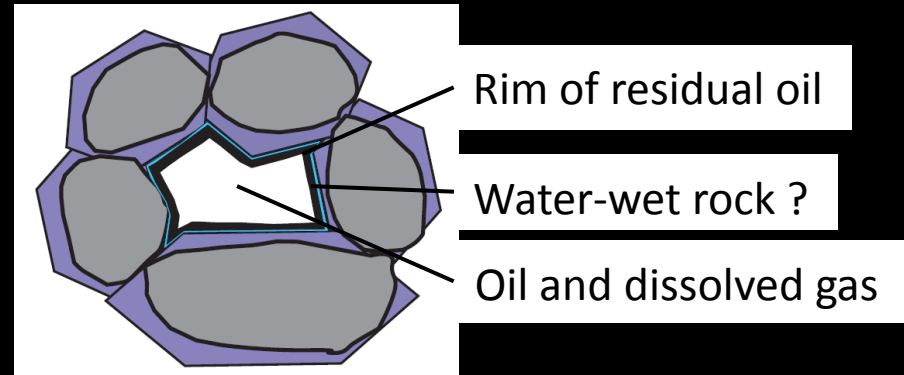
- **Mineral pores**

- Primary mineral pore
 - Interparticle pore
 - Intraparticle pore
- **Modified mineral pore**



- **OM pores**

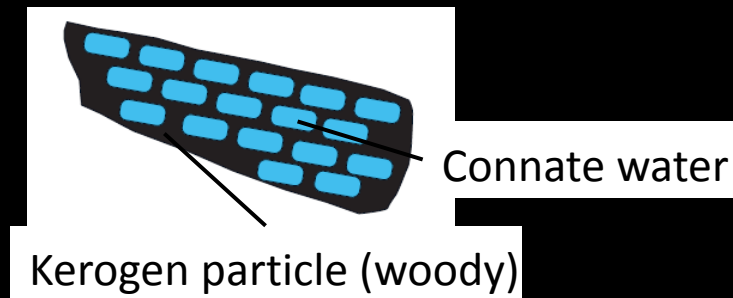
- Primary OM pore
- Secondary OM pore
 - OM bubble pore
 - OM spongy pore



Define and Categorize EF Pore Types

- **Mineral pores**
 - Primary mineral pore
 - Interparticle pore
 - Intraparticle pore
 - Modified mineral pore

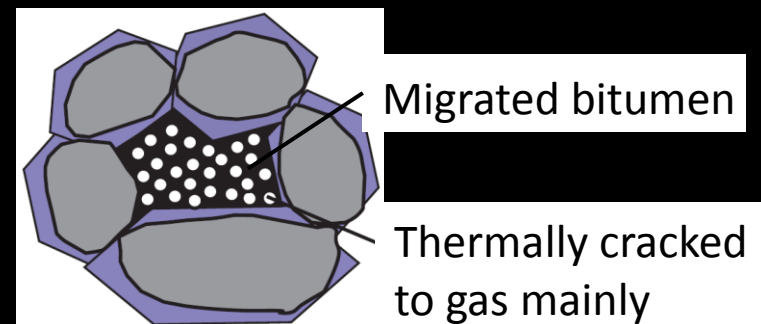
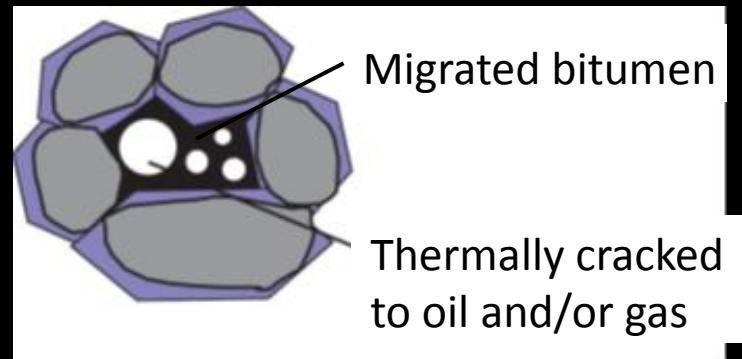
- **OM pores**
 - **Primary OM pore**
 - Secondary OM pore
 - OM bubble pore
 - OM spongy pore



Define and Categorize EF Pore Types

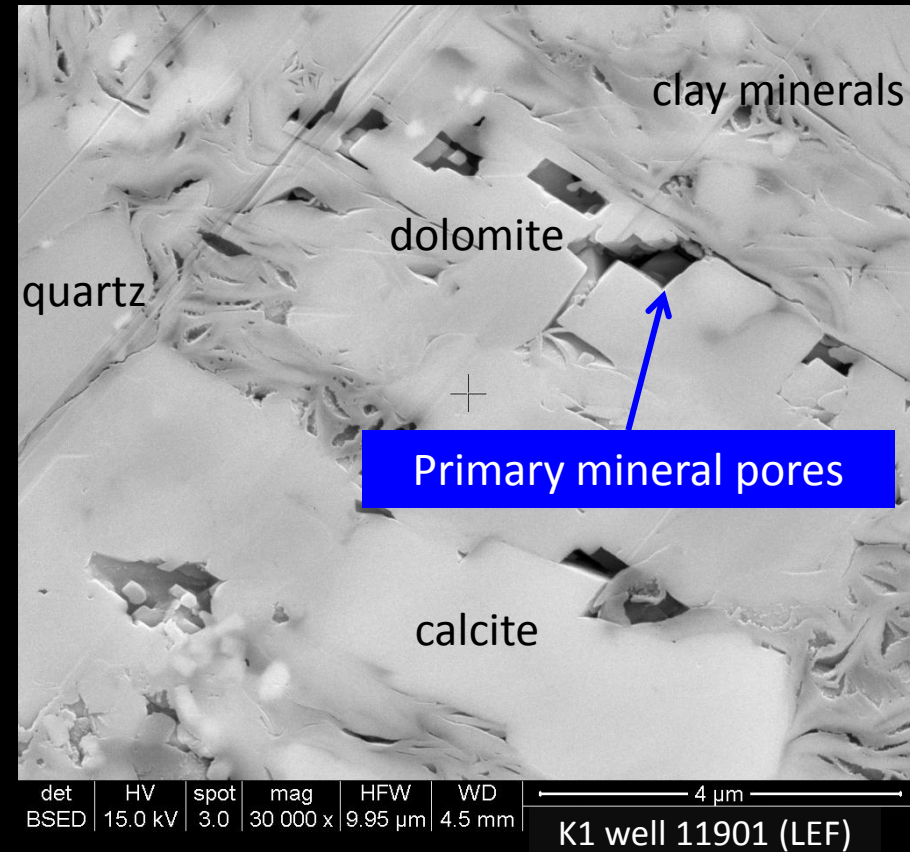
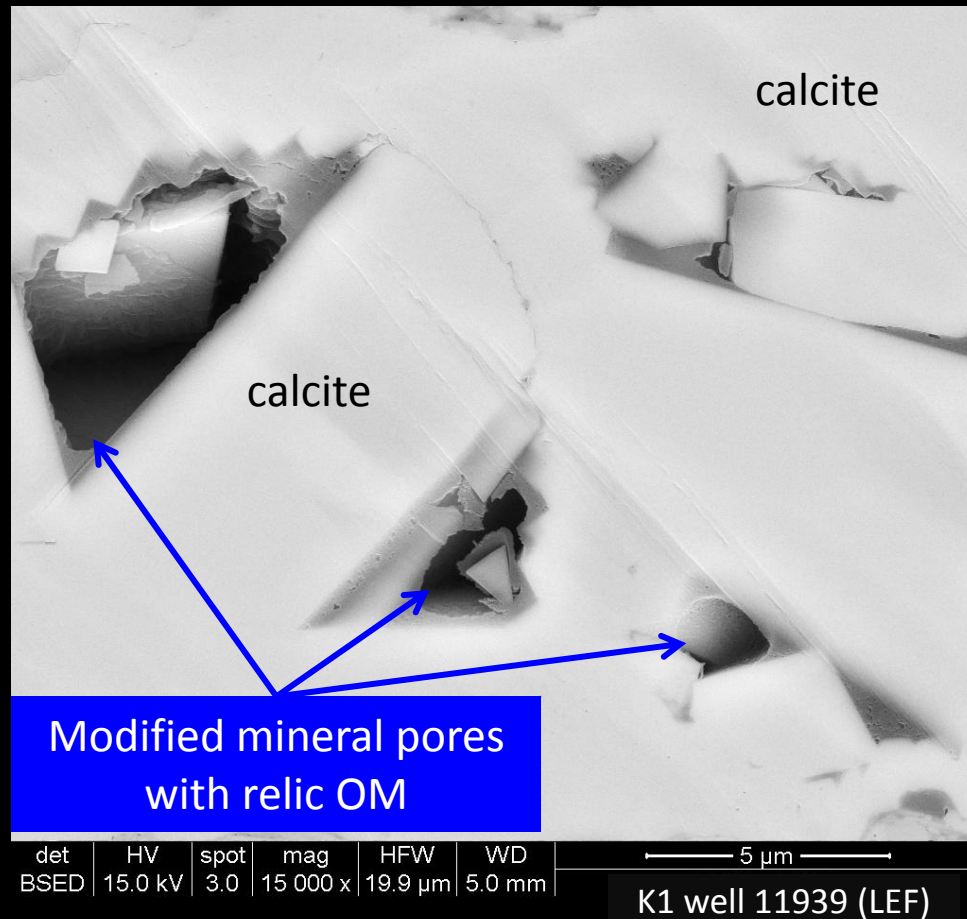
- **Mineral pores**
 - Primary mineral pore
 - Interparticle pore
 - Intraparticle pore
 - Modified mineral pore

- **OM pores**
 - Primary OM pore
 - **Secondary OM pore**
 - OM bubble pore
 - OM spongy pore



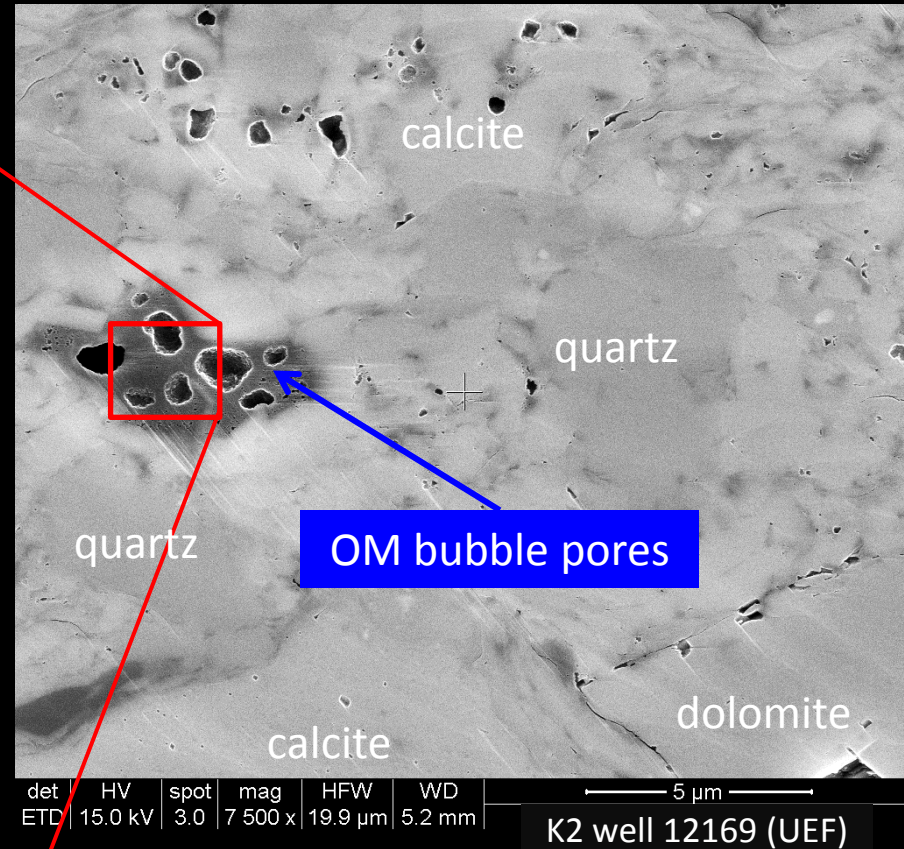
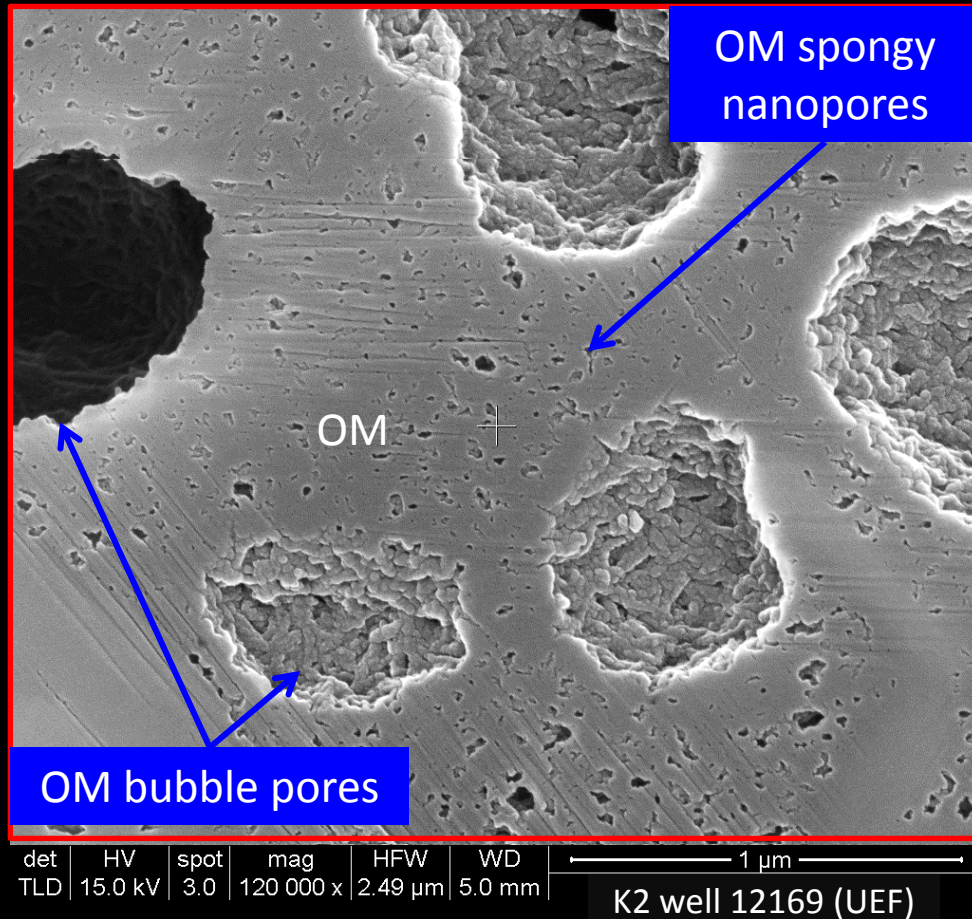
Examples of Dominant Mineral Pores

- SEM photomicrographs showing
 - (1) Modified mineral pores
 - (2) Primary mineral pores

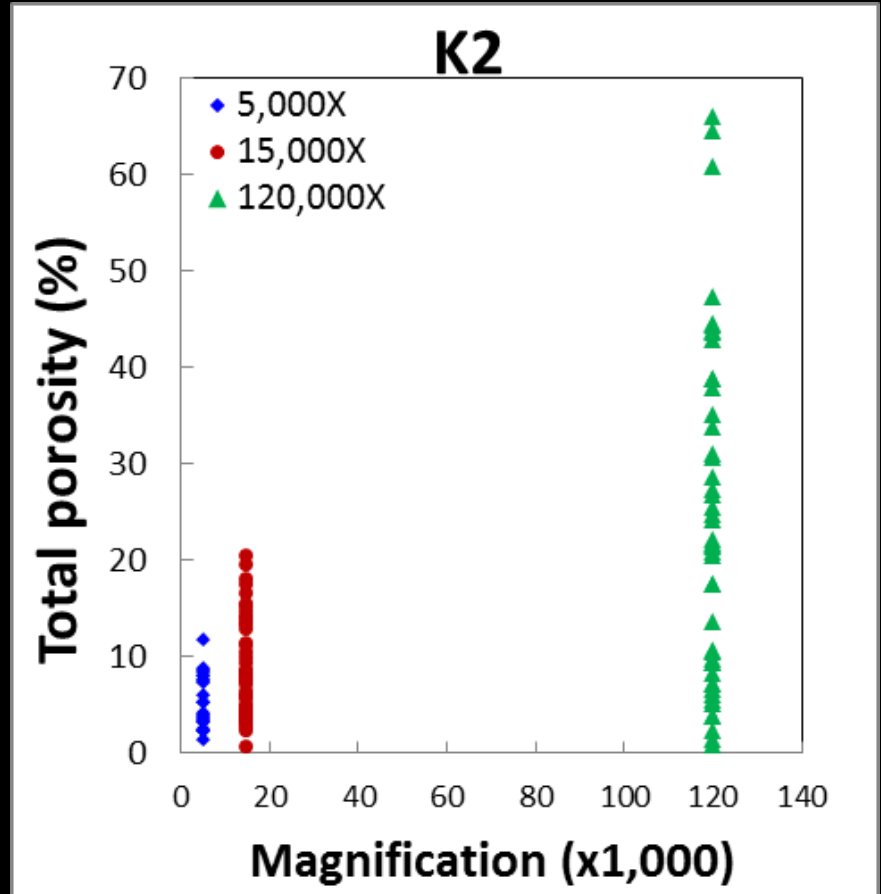
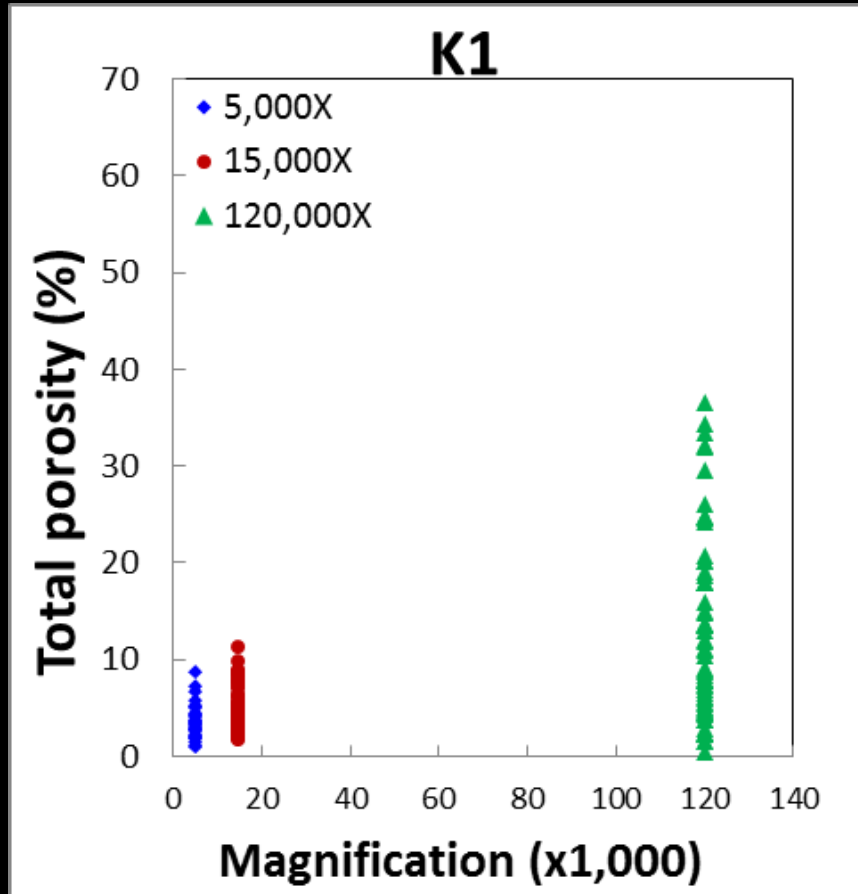


Examples of Dominant OM Pores

- SEM photomicrographs showing
 - (1) OM bubble pores
 - (2) OM spongy pores



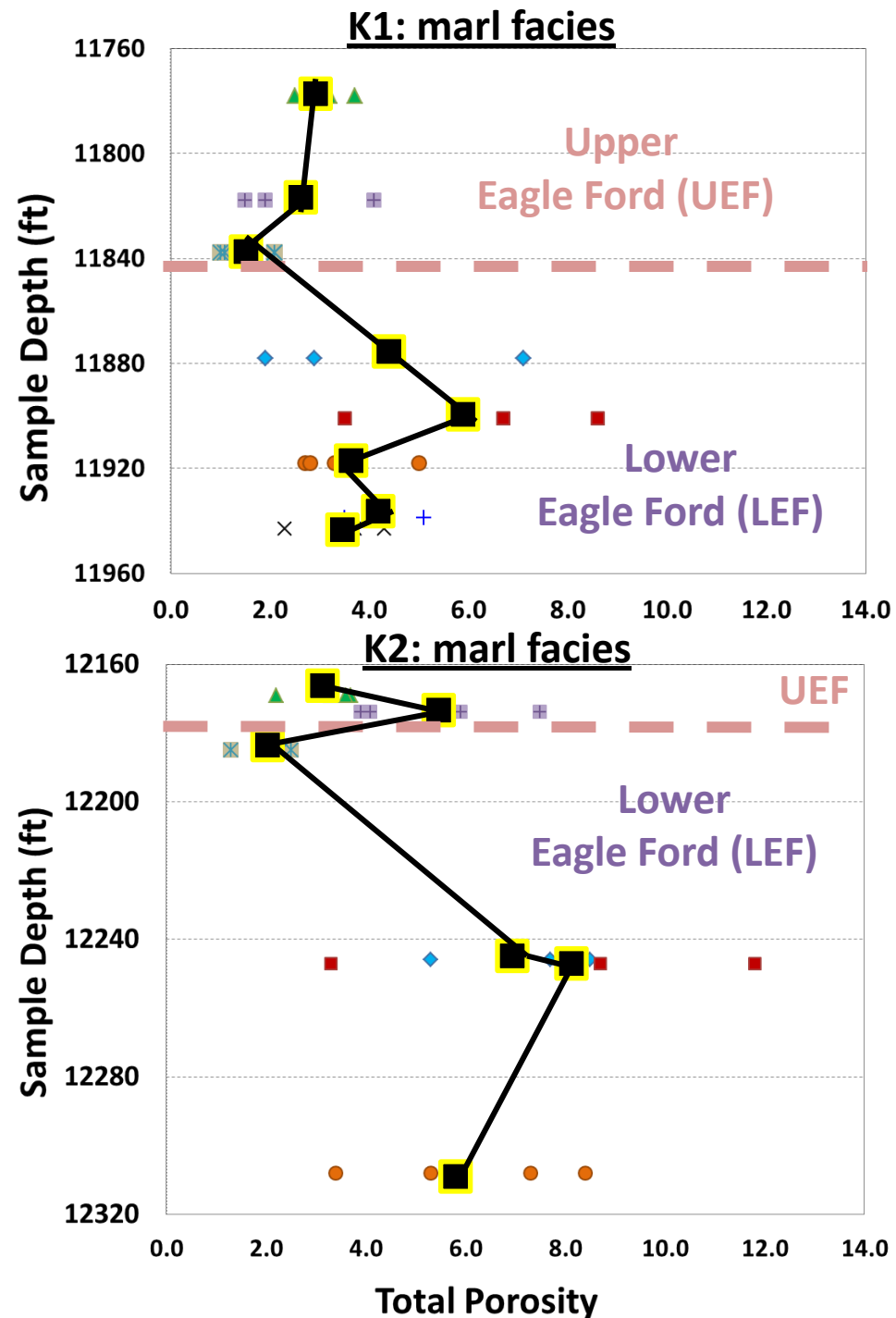
Total Visible Porosity at Different Scales



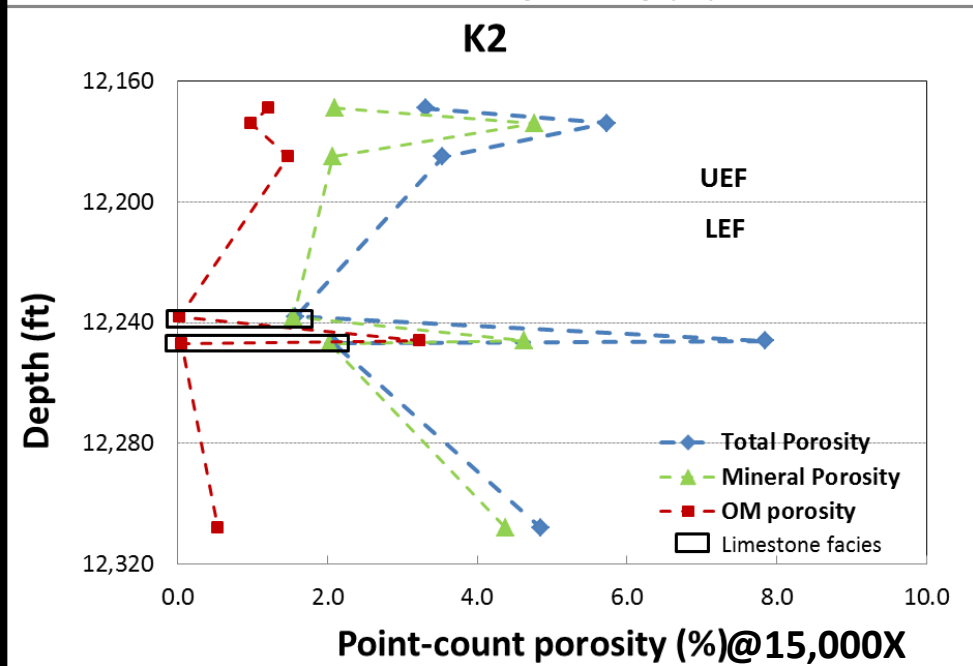
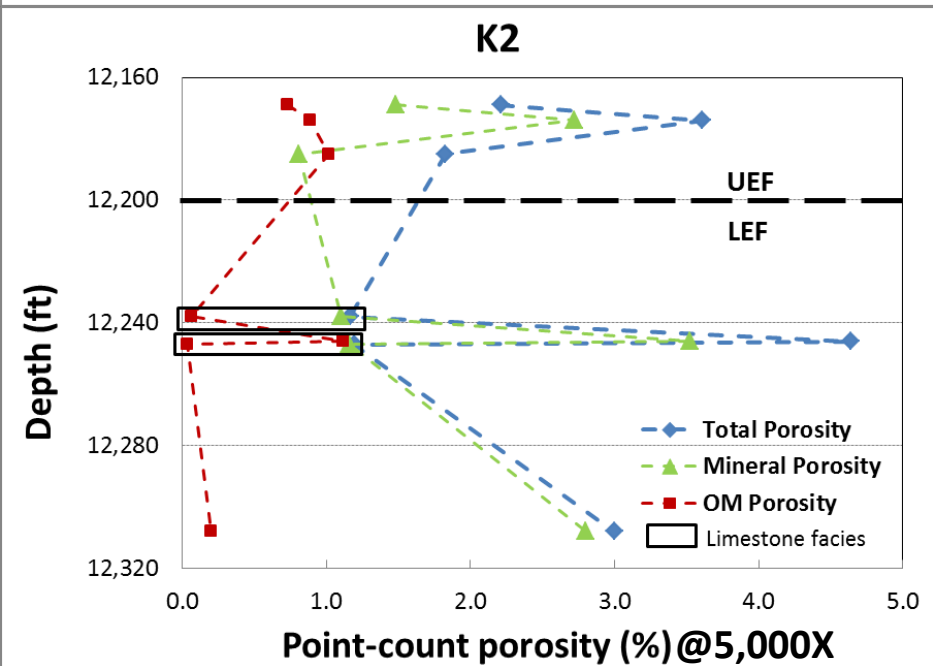
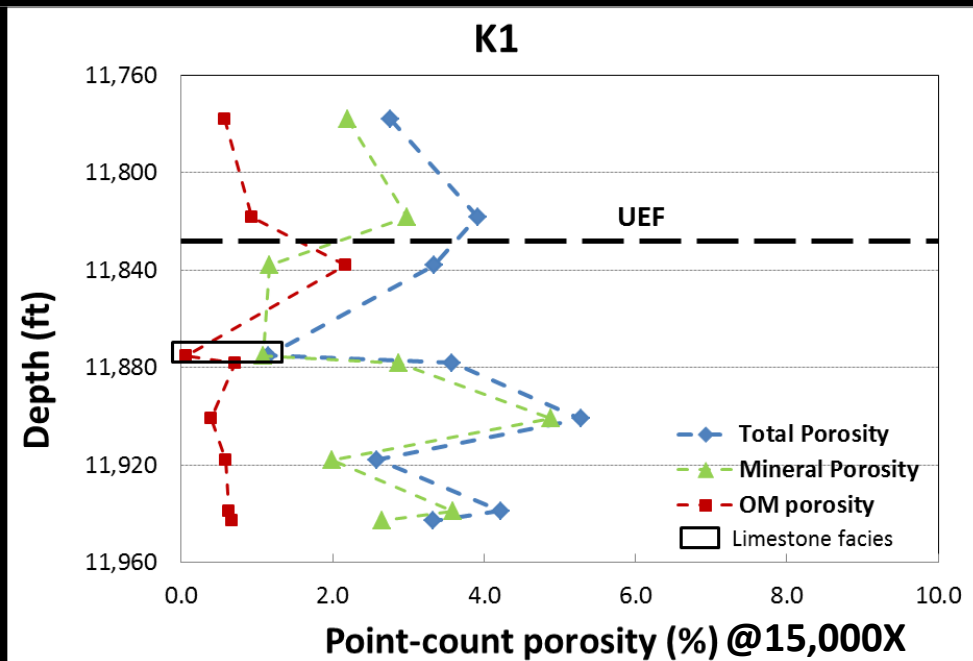
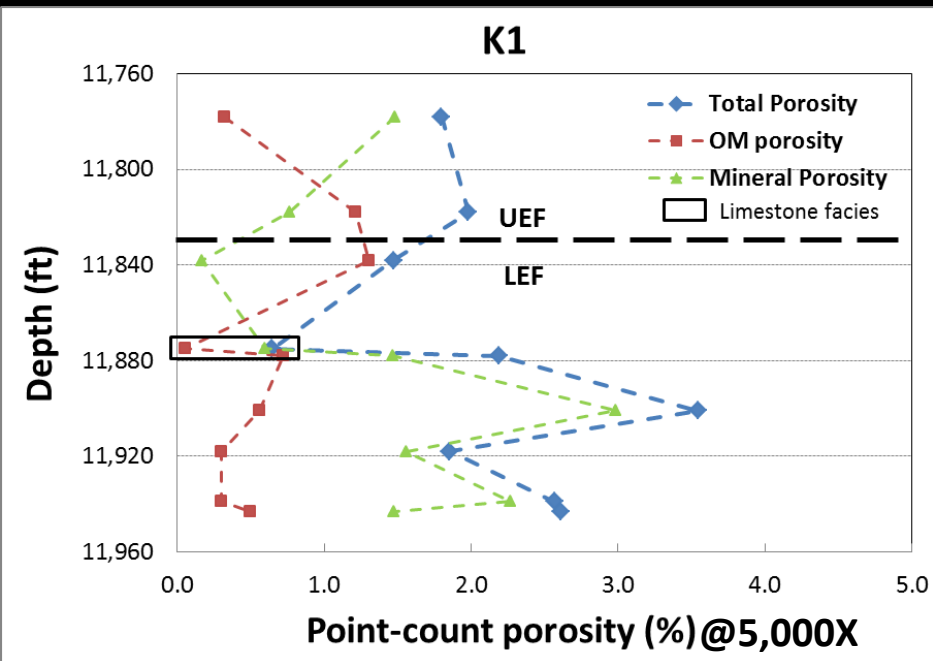
- Visible point-count porosity increases towards higher magnification images because smaller pores are best resolved at 120,000X
- However, areas at highest magnification are the least representative

Sample Depth vs. Total Porosity (5,000X)

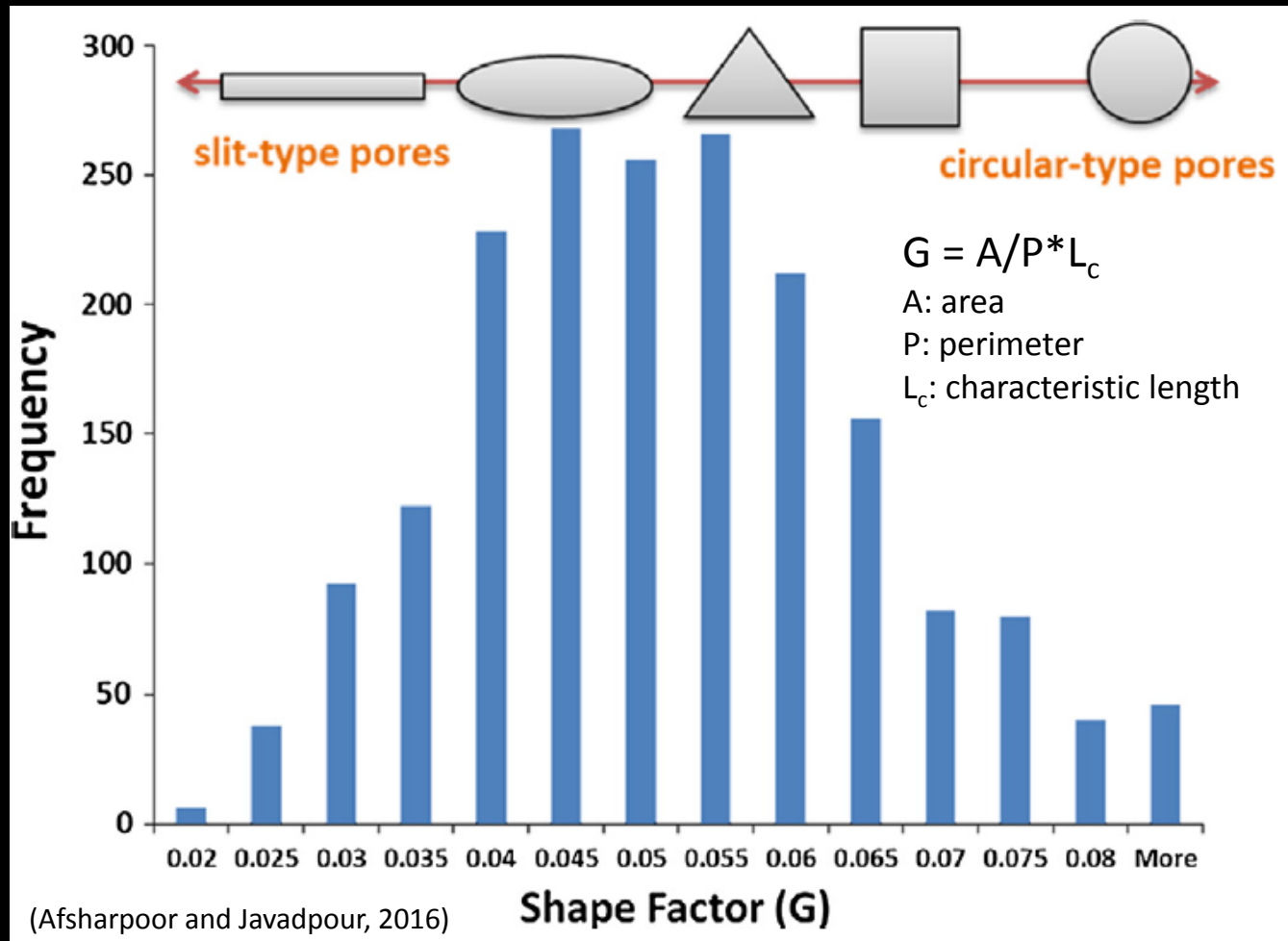
- Extent of spreading of the data points implies the heterogeneity of rocks
- Average visible porosity in marls marked in black
- Average visible porosity increases towards LEF



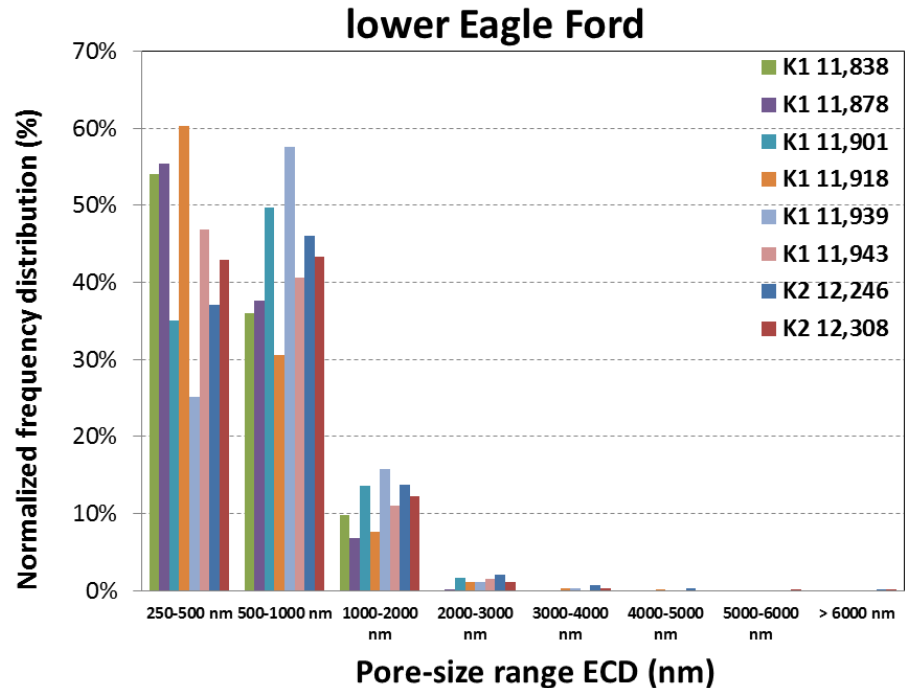
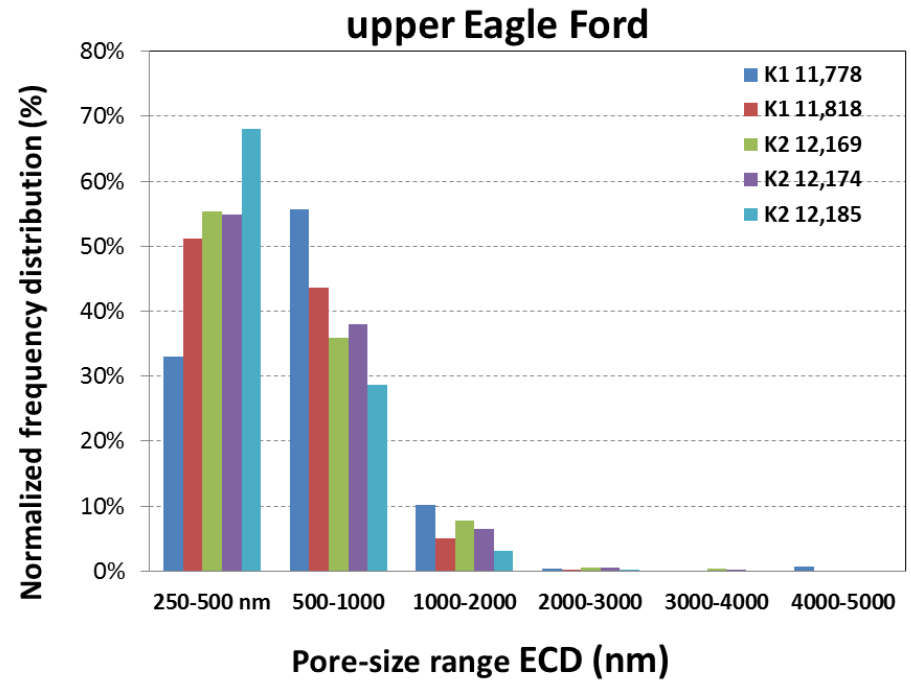
Mineral Pores Dominate EF Pore Network



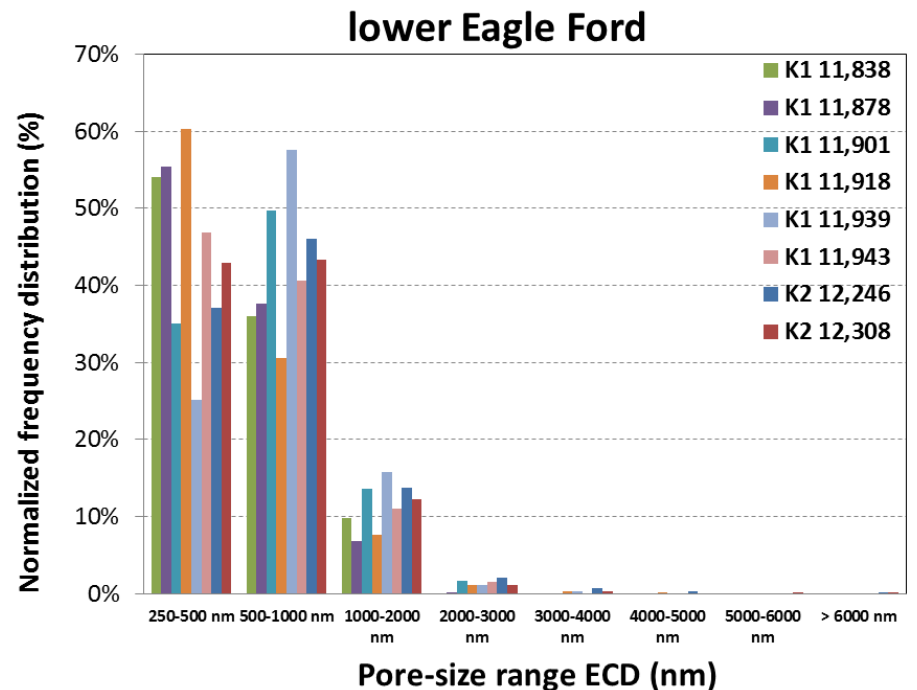
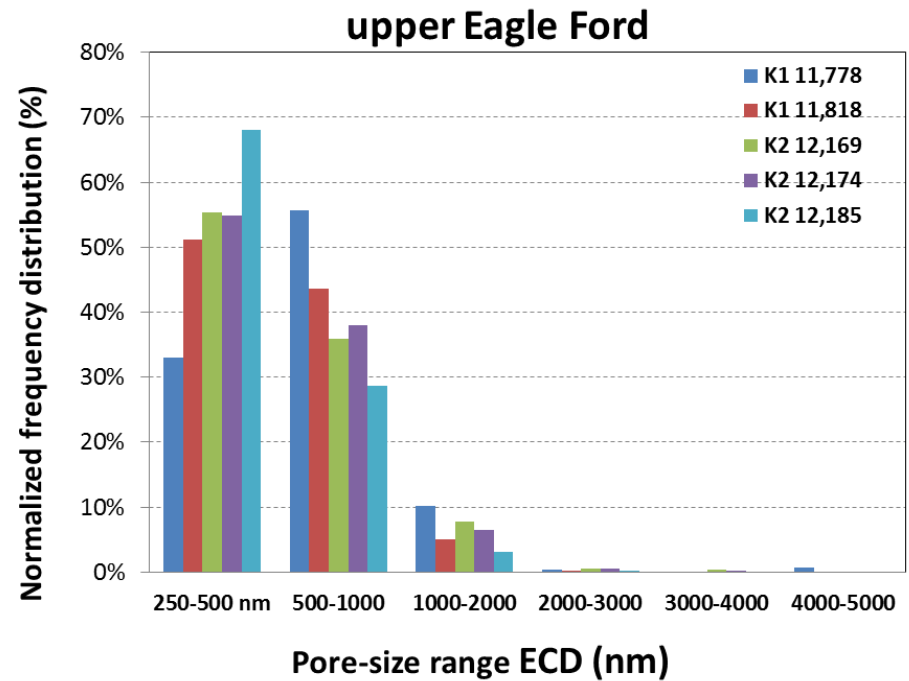
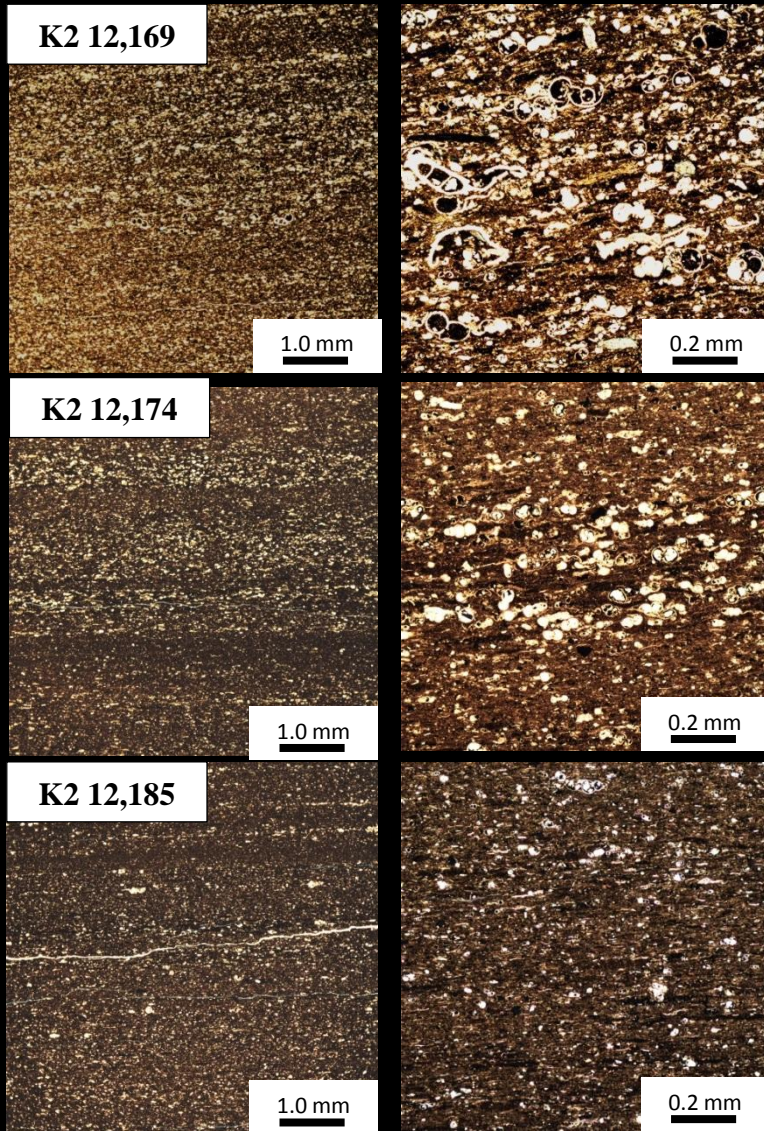
Pore Shape, Pore-Size Distribution



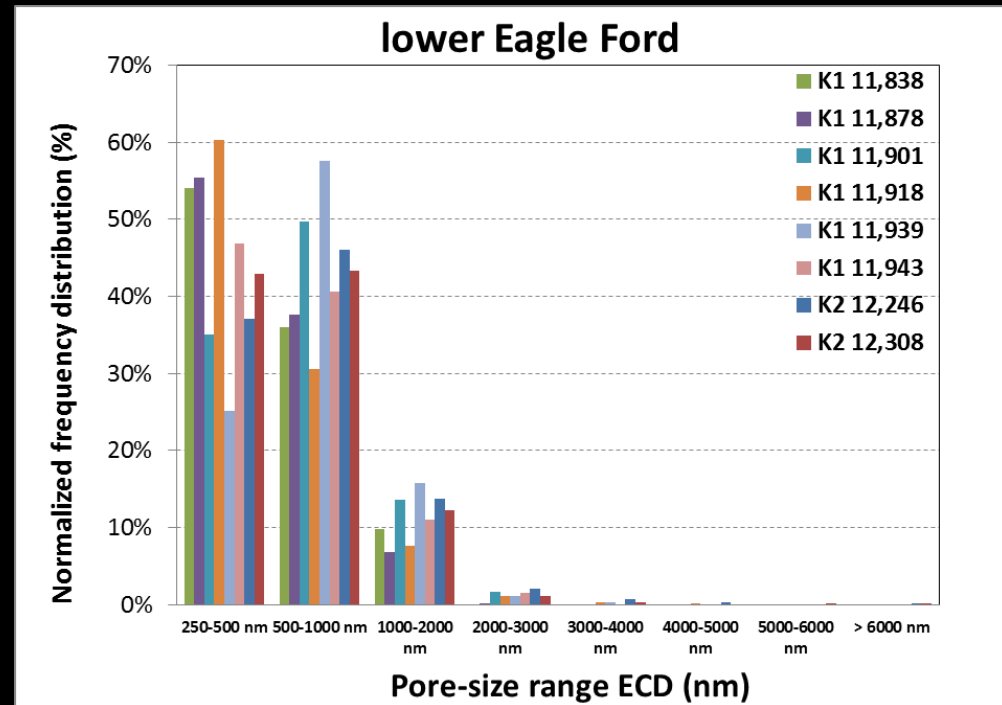
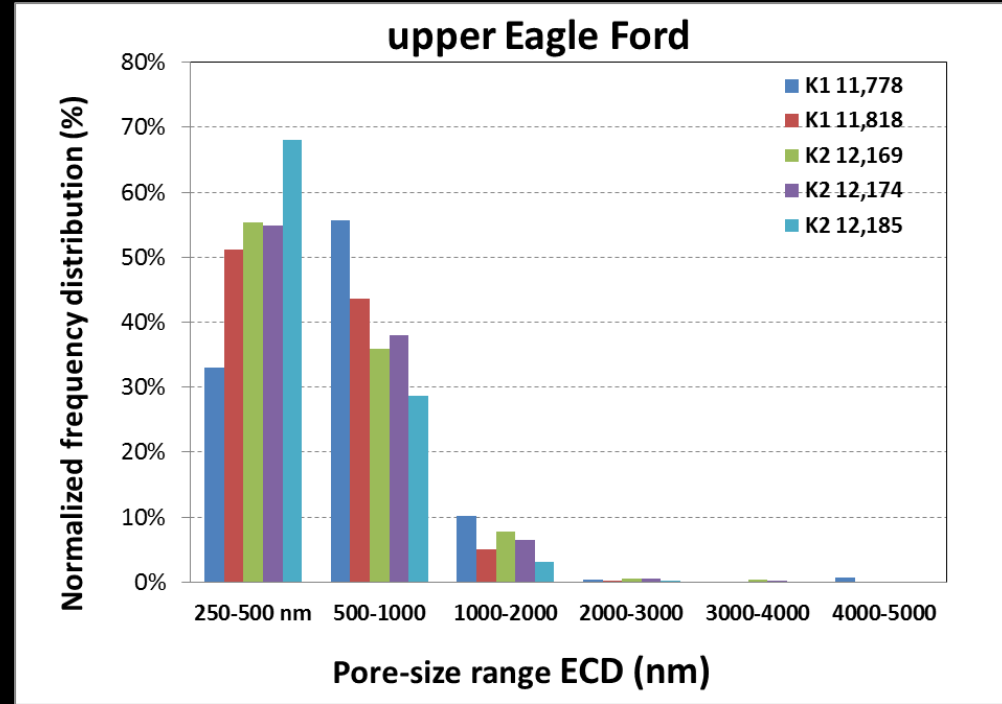
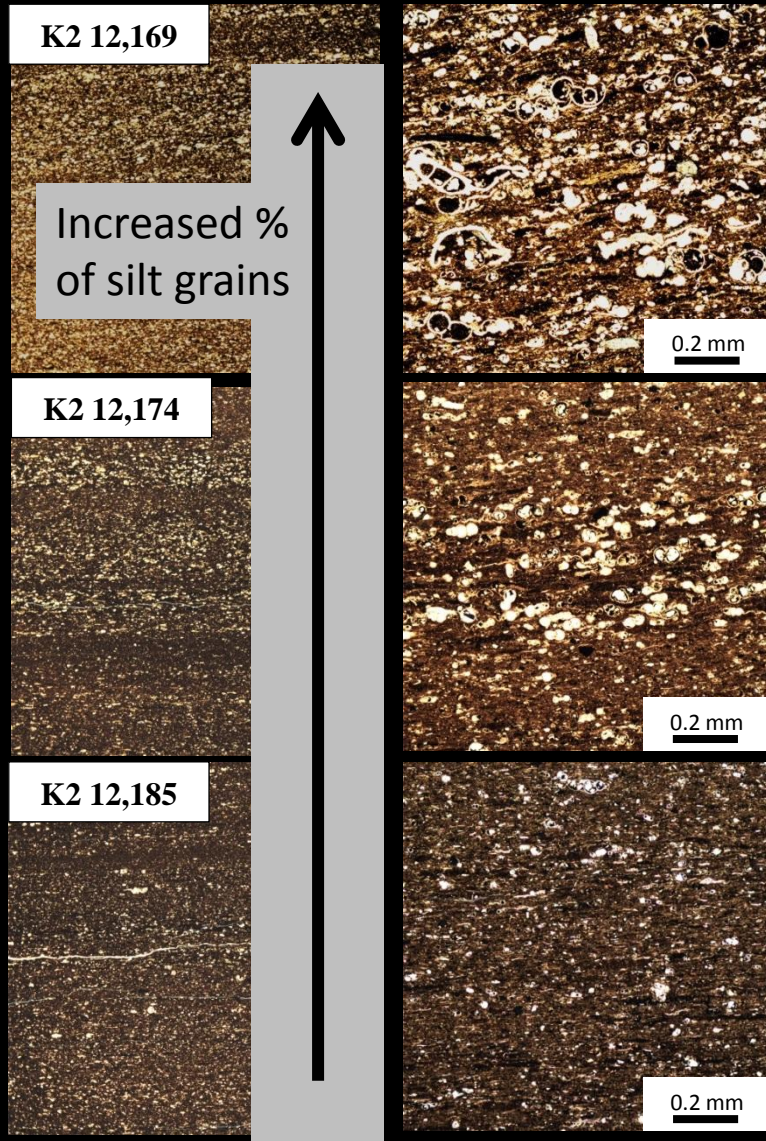
Pore Shape, Pore-Size Distribution



Pore Shape, Pore-Size Distribution

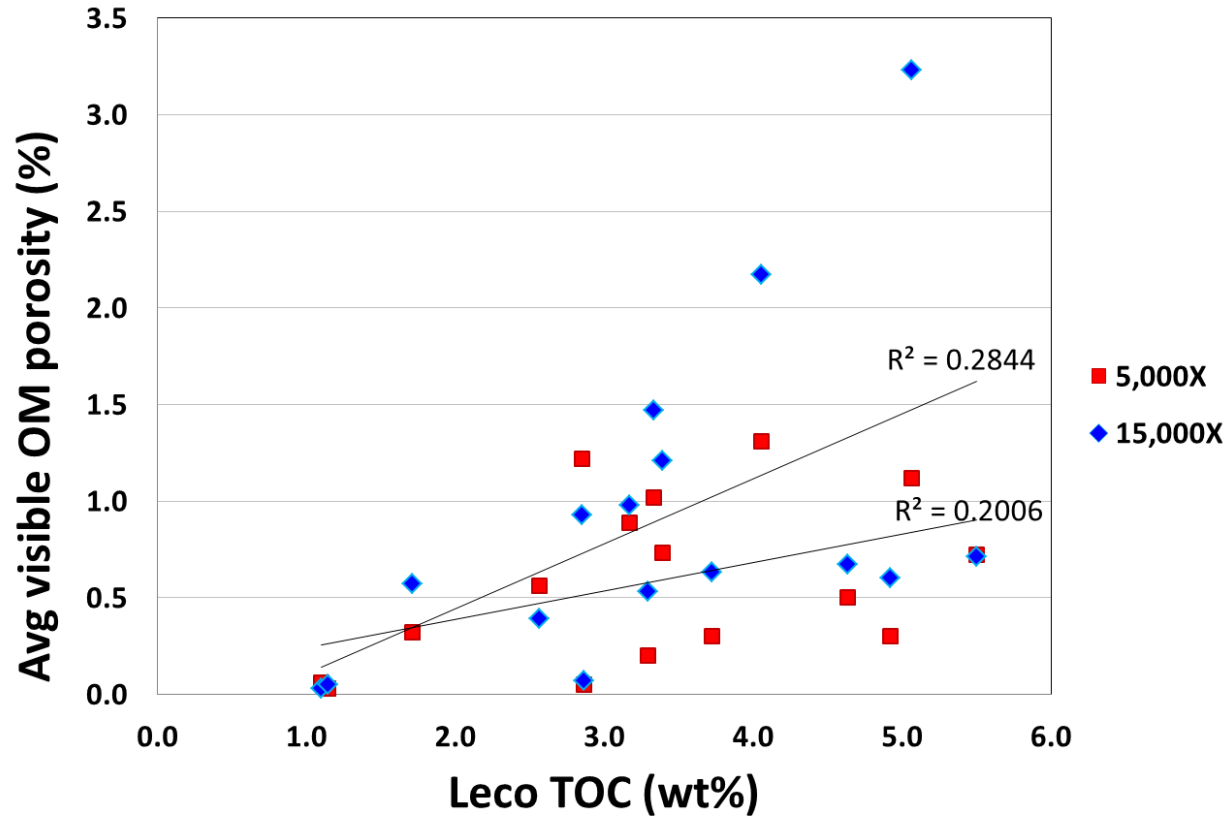


Pore Shape, Pore-Size Distribution



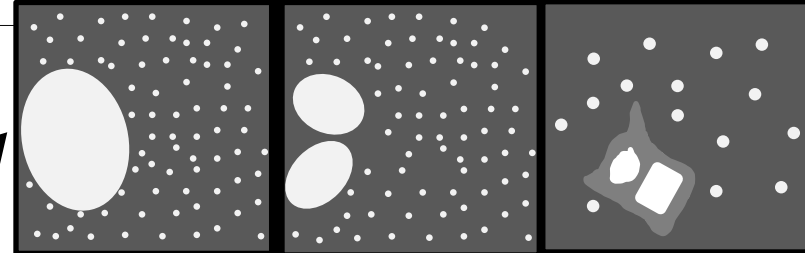
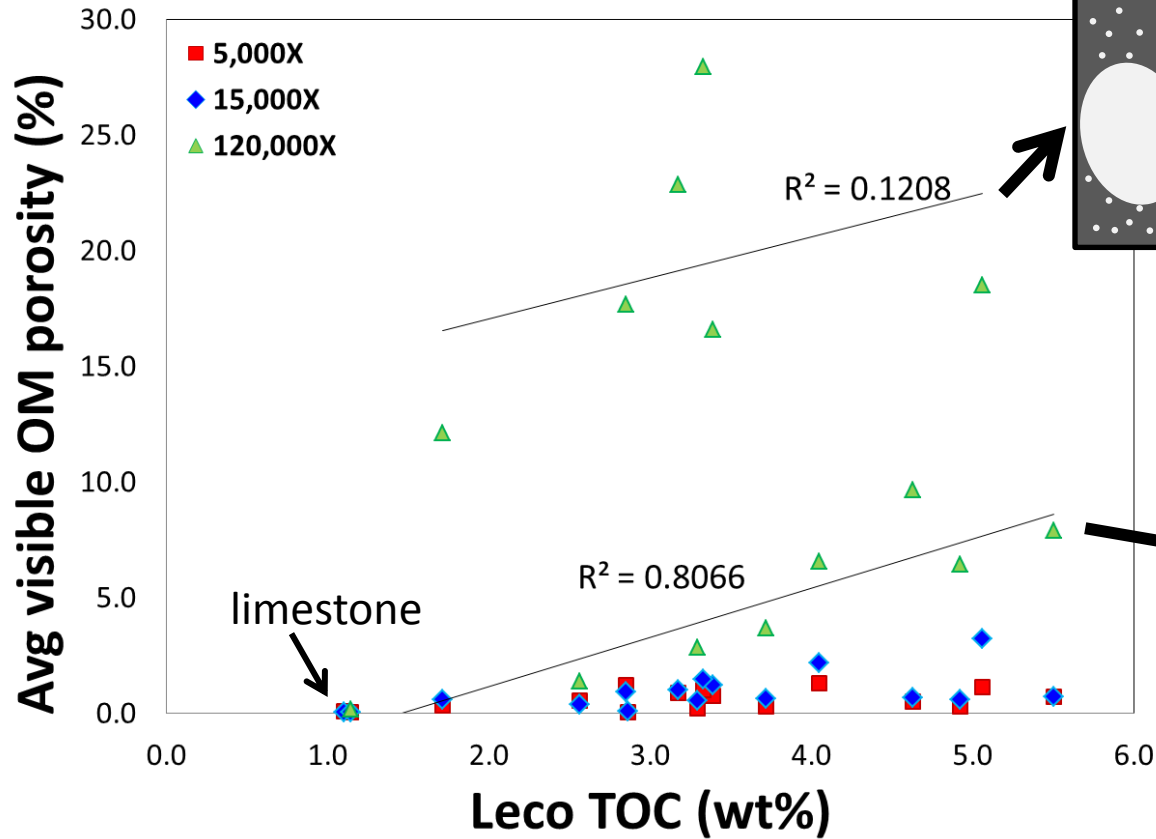
Impacts of TOC on OM Porosity

Average visible OM porosity vs. TOC

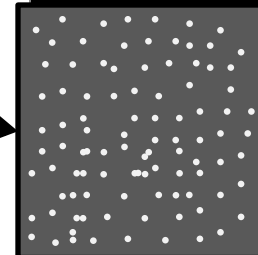


Impacts of TOC on OM Porosity

Average visible OM porosity vs. TOC



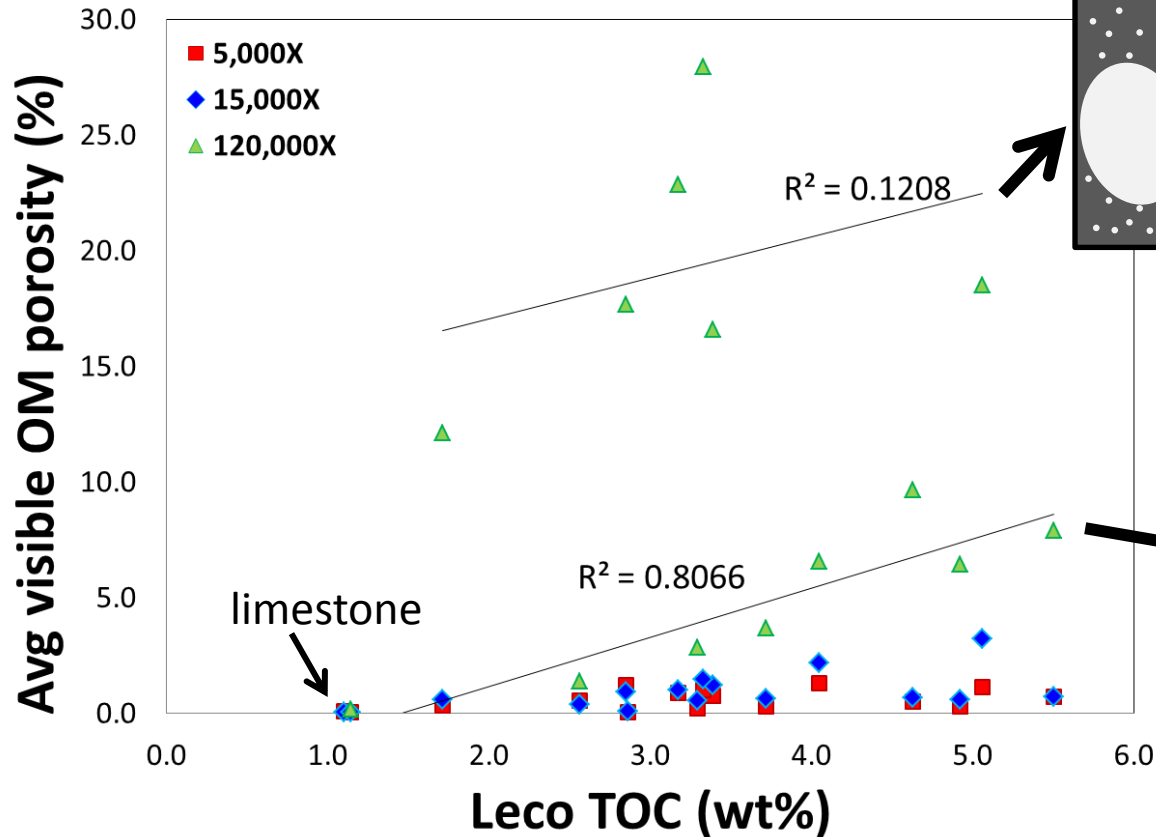
OM bubble + spongy pores + primary OM pores



OM spongy pores

Impacts of TOC on OM Porosity

Average visible OM porosity vs. TOC



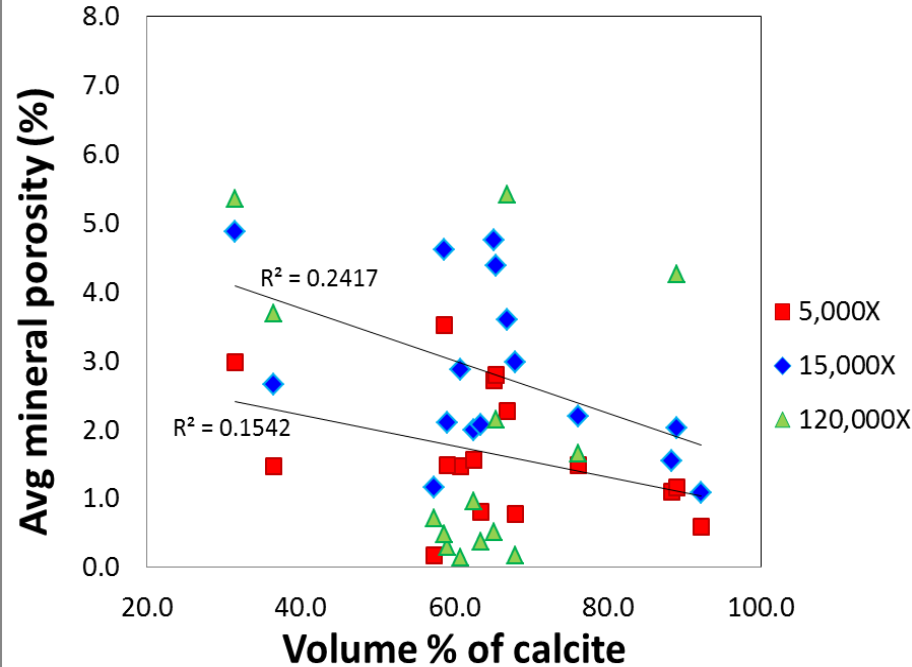
OM bubble + spongy pores + primary OM pores

OM spongy pores

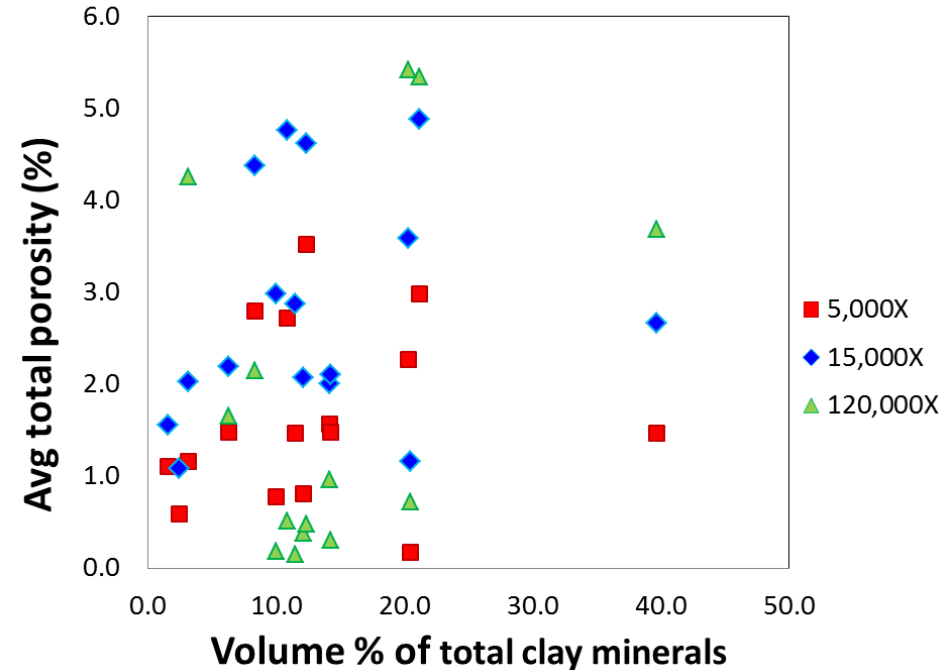
- **Positive correlation** for total **OM spongy porosity** with **TOC**
- Likely multiple factors determine distribution of OM porosity, not just TOC

Calcite, Total Clay Minerals vs. Mineral Porosity

Average mineral porosity vs. calcite

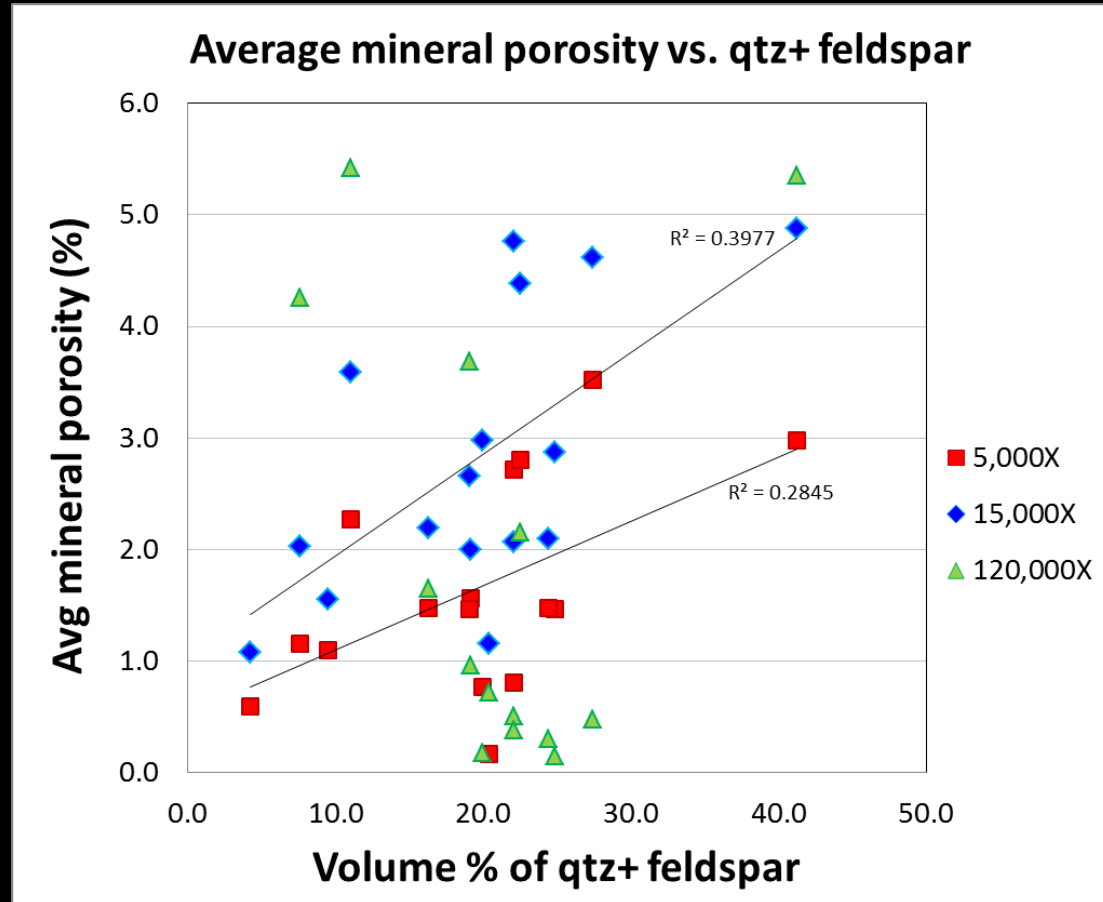


Average mineral porosity vs. total clay



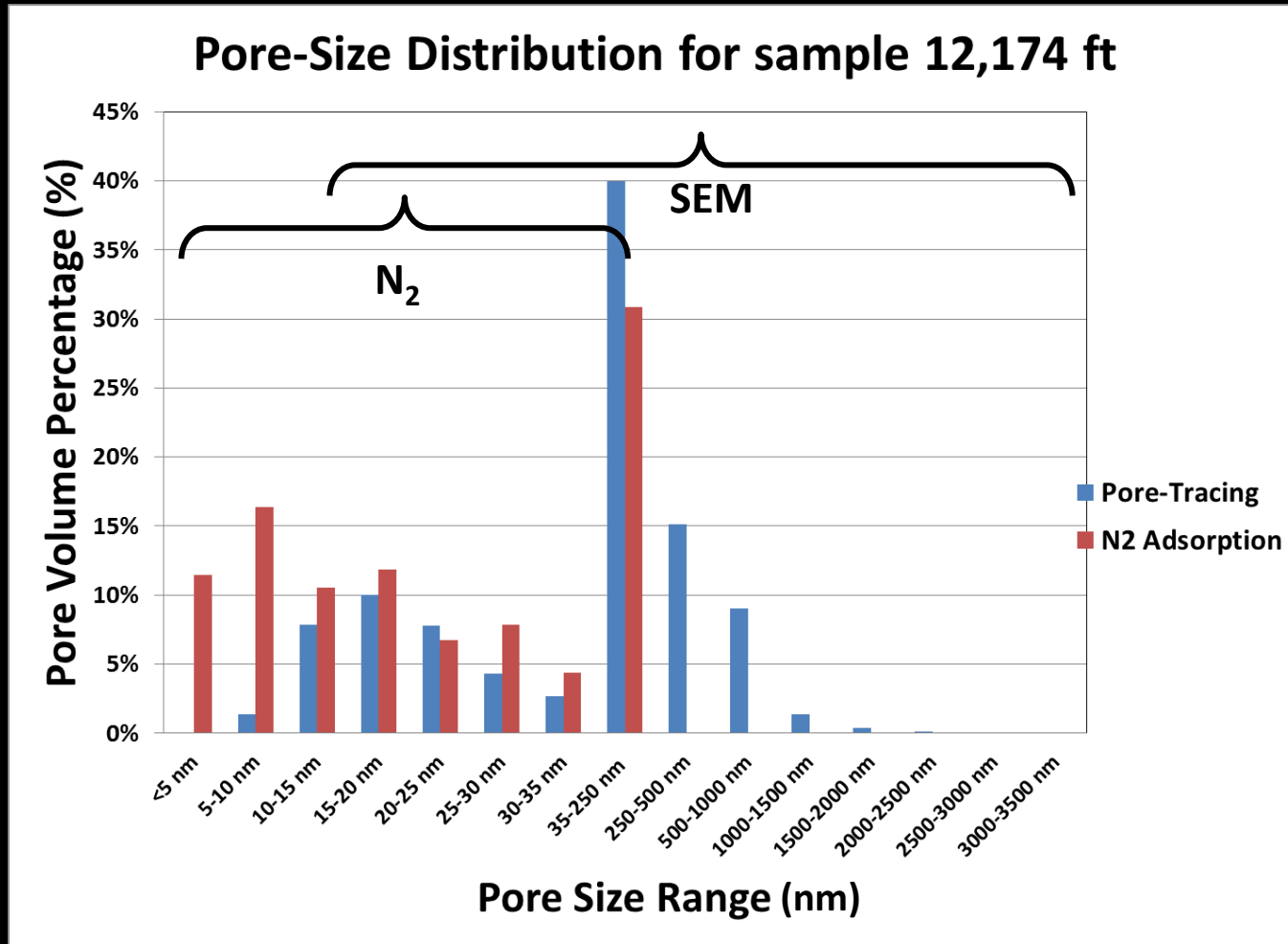
- No correlation for mineral porosity vs. calcite and total clay minerals vol.%
- Although concentrated areas of fecal pellets (composed of coccolith hash) and broken foraminifera bodies are major allochems that host interparticle pores -> calcite is also cement

(Quartz + Feldspar) vs. Mineral Porosity



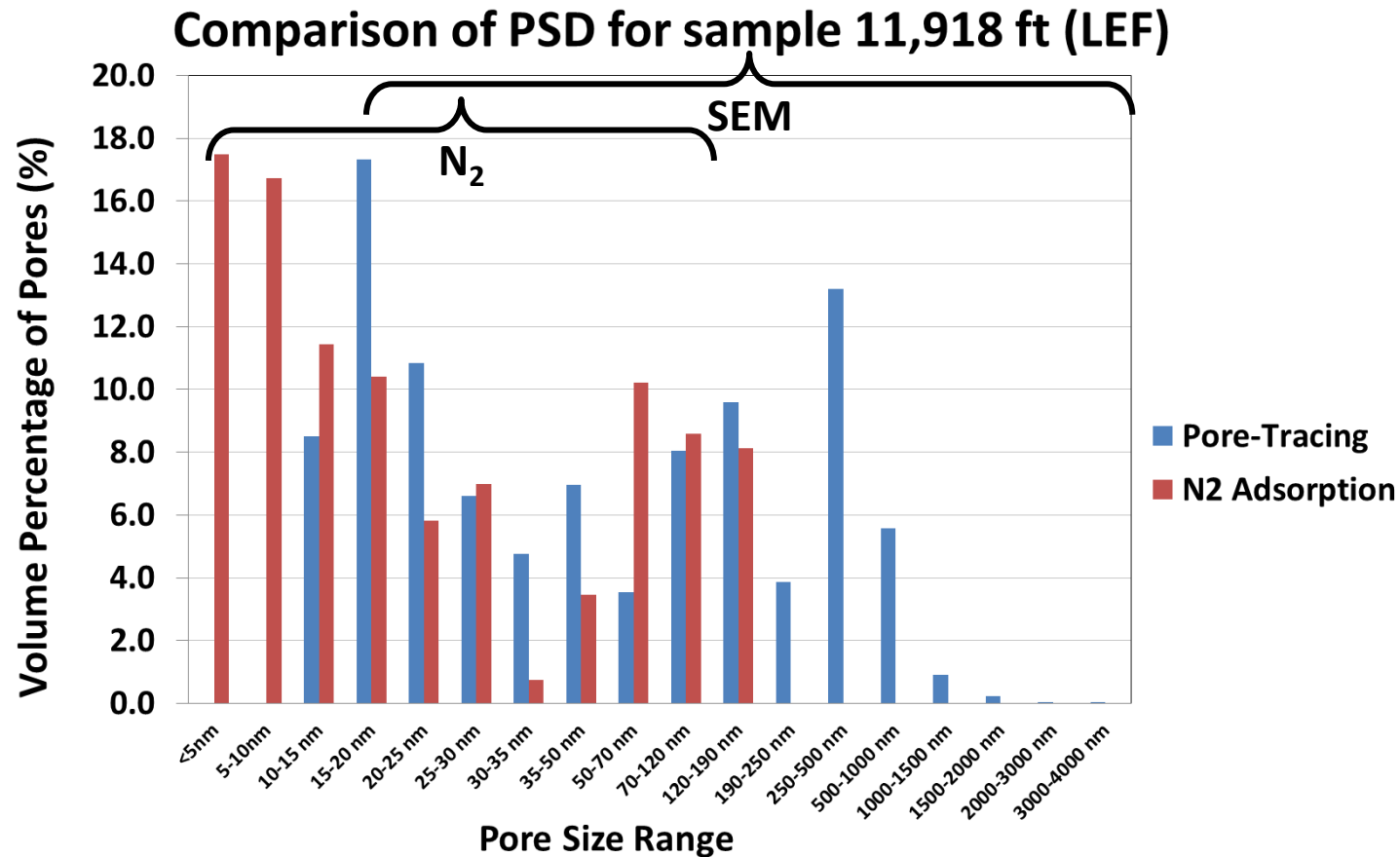
- Weak positive correlation for mineral porosity vs. quartz + feldspars vol.%
- Interpreted to be related to the rigidity of the mineral framework that inhibits compaction of mineral pores and later allowed petroleum to migrate within the intergranular pore networks

Compare Pore-Size Distribution



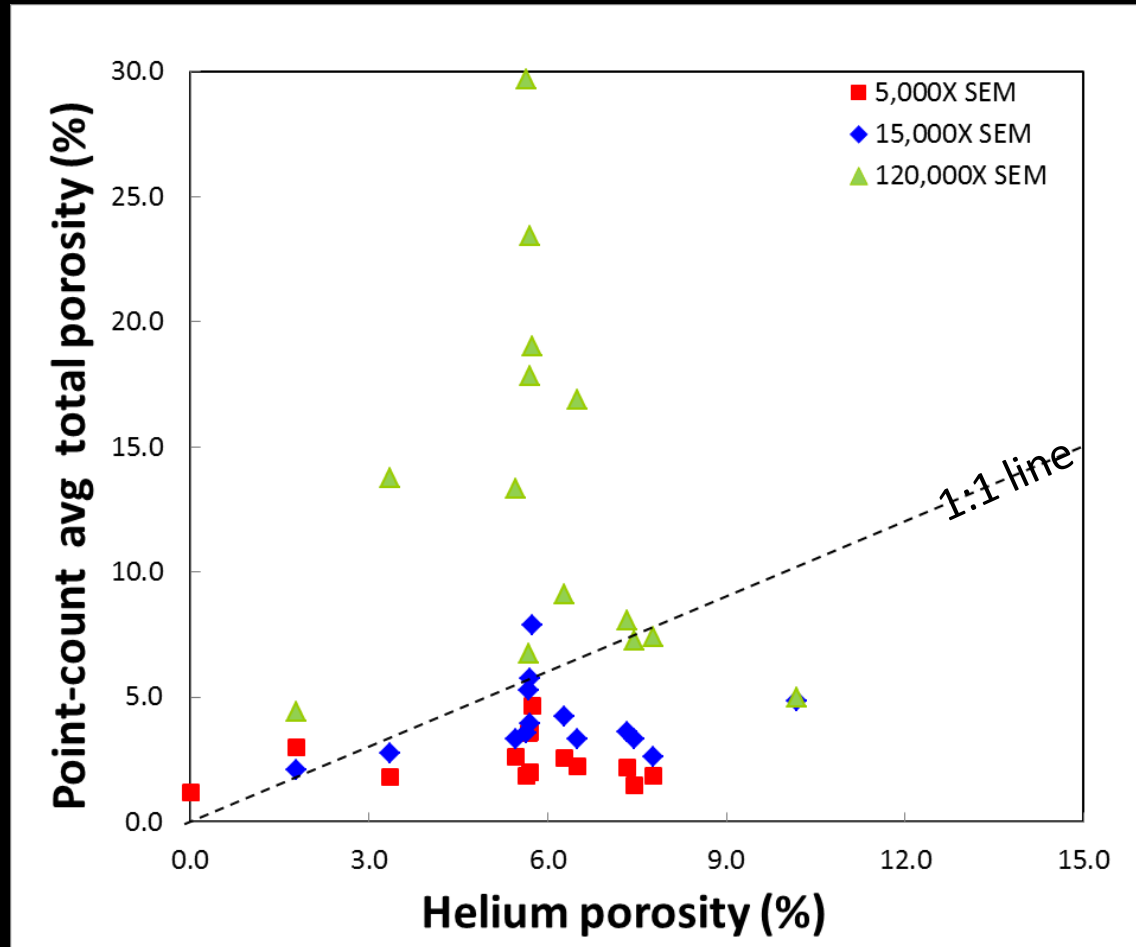
- PSD derived from SEM imaging and N2 adsorption is straightforward in comparison
- Pores > 250 nm is approximately 25% of the total pore volume (SEM)

Compare Pore-Size Distribution



- Some inconsistency for pores in the 30- to 70-nm size range
- Data raises some concerns regarding the reliability of either method

Compare image-based and He porosity



- SEM image-based porosity underestimates the bulk porosity because pores less than 5 nm are not included (cannot be resolved)
- However, SEM provides pore type and network information that other methods cannot provide

Conclusions

- Mineral pores and their pore networks are main contributor to total porosity and total pore network in the EF strata
- Pore development is primarily controlled by depositional and diagenetically modified processes (first order) and thermal maturation of organic matter (second order): compaction & cementation are two important processes in the EF
- Bulk mineralogy of UEF marls is similar; however, LEF marls demonstrate much more variations: increase abundance of kaolinite and chlorite and significant diagenetic alteration observed in LEF

Conclusions

- OM pore morphology affects OM porosity. Only OM spongy pore volume relates to TOC.
- Strong nm- and μm - scale heterogeneity of rock components and properties (texture, fabric, mineralogy, and TOC) affects pore types, abundance, and distribution – without complication of thermal maturity

Implication and Future Works

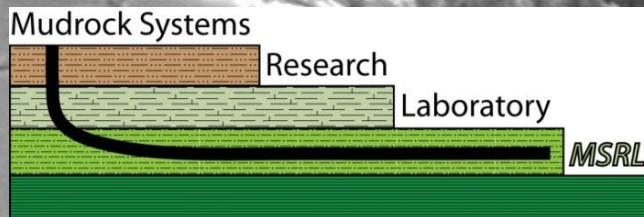
- Texture and fabric impact pore-size distribution. Quantification of grain size, shape, and sorting is needed.
- Quantification of diagenesis in mudstones. Relationship of compaction and cementation of mudstone is not clear.
- Identification of kerogen and pyrobitumen using synchrotron-based scanning transmission X-ray microscopy (STXM) or other advanced techniques
- Can we connect these quantitative results to petrophysics? If so, what will be the representative elemental area (REA)?

Acknowledgement

- Marathon Oil Company
- Joan Spaw
- Athma Bhandari
- Farzam Javadpour
- Kitty Milliken
- Robert Reed
- Xun Sun
- Patrick Smith
- MSRL member sponsors
- K-T GeoServices, Inc.
- STARR (State of Texas Advanced Oil and Gas Resource Recovery) program



BUREAU OF
ECONOMIC
GEOLOGY



TEXAS Geosciences
The University of Texas at Austin
Jackson School of Geosciences